

PERFORMANCE ANALYSIS OF SPACE-TIME CODES

APPROVED BY SUPERVISORY COMMITTEE:

---

Dr. Aria Nosratinia, Chair

---

Dr. John Fonseca

---

Dr. Kamran Kiasaleh

---

Dr. Mohammed Saquib

Copyright 2003

Harsh P. Shah

All Rights Reserved

To My Parents

PERFORMANCE ANALYSIS OF SPACE-TIME CODES

by

HARSH P. SHAH, B.E.

THESIS

Presented to the Faculty of  
The University of Texas at Dallas

in Partial Fulfillment  
of the Requirements  
for the Degree of

MASTER OF SCIENCE IN ELECTRICAL ENGINEERING

THE UNIVERSITY OF TEXAS AT DALLAS

December 2003

## ACKNOWLEDGEMENTS

I thank my advisor Dr. Aria Nosratinia for providing me with the opportunity to work as graduate student with him. I express my gratitude to Dr. Nosratinia for his guidance, support and confidence he has shown in my work. I also thank him for instilling a sense of curiosity to learn new things in me.

I am thankful to thank Dr. Fonseka, Dr. Mohammed Saquib and Dr. Kiasaleh for serving on my supervisory committee. I express my gratitude for their helpful suggestions and comments that assisted me in improving the presentation of this thesis.

I would like to thank Ahmadreza Hedayat for helping me and guiding me throughout my research. I would also like to thank my other colleagues of the Multimedia Communications Laboratory, Mohammad, Ramky, Todd, Shahab and Vijay for their timely help and support.

I would like to thank my family for their constant encouragement and support.  
December 2003.

# PERFORMANCE ANALYSIS OF SPACE-TIME CODES

Harsh P. Shah, M.S.E.E.

The University of Texas at Dallas, 2003

Supervisor: Dr. Aria Nosratinia

Multiple-input multiple-output systems have better performance under fading channels than single-input single-output (SISO) systems. Previous analyses of these systems concentrate on uncorrelated antennas. However, antenna spacing and properties of scattering environment, among other things, can create correlation between channel coefficients. Furthermore, for various reasons one may not be able or willing to fully interleave the codewords, therefore there may exist temporal correlation between fading coefficients. Existing analyses often assume that the fading is either quasi-static or i.i.d. This work presents a comprehensive analysis of MIMO systems under correlated fading. We provide analysis that applies to all space-time codes under arbitrary channel conditions. We also present analysis for the special case where space-time block codes are concatenated with channel codes. We calculate pairwise error probability (PEP) expressions under quasi-static fading, fast fading, block fading, as well as arbitrarily temporally correlated fading, under Rayleigh and Rician conditions. We then use this PEP expressions to calculate union bounds on the performance of space-time codes. Simulations verify accuracy of our results.

## TABLE OF CONTENTS

Acknowledgements	v
Abstract	vi
List of Figures	ix
Chapter 1. Introduction	1
1.1 Wireless communications . . . . .	1
1.2 Literature review . . . . .	4
1.3 Scope and outline of the thesis . . . . .	5
Chapter 2. Overview of space-time signaling	7
2.1 Multiple-input multiple-output (MIMO) channels . . . . .	7
2.2 Diversity techniques . . . . .	9
2.2.1 Transmit diversity and space-time block codes . . . . .	11
2.2.2 Space-time trellis codes . . . . .	13
2.2.3 Super-orthogonal space-time codes . . . . .	15
2.2.4 Linear-dispersion codes . . . . .	17
2.3 Further reading . . . . .	18
Chapter 3. Analytical tools	19
3.1 Spatially correlated channel . . . . .	19
3.2 Union bounds on frame and bit error probability . . . . .	20
3.3 Alternative expression for Q function . . . . .	22
Chapter 4. Analysis of space-time codes	24
4.1 System model . . . . .	24
4.2 Quasi-static fading with spatial correlation . . . . .	26
4.3 Fast fading with spatial correlation . . . . .	28
4.4 Block fading with spatial correlation . . . . .	29

4.5	Temporal and spatial correlation . . . . .	30
4.6	Performance under Rician fading . . . . .	32
4.7	Summary . . . . .	33
Chapter 5. Analysis of coded space-time block transmission		34
5.1	System model . . . . .	34
5.2	Analysis of block fading channel . . . . .	37
5.3	PEP based on moment generating functions . . . . .	39
5.4	Independent fading . . . . .	40
5.5	Spatially correlated fading . . . . .	41
5.6	Temporal and spatial correlation . . . . .	42
5.7	Performance analysis with multilevel modulation . . . . .	44
5.8	Performance under Rician fading . . . . .	47
5.9	Summary . . . . .	48
Chapter 6. Applications and results		49
6.1	Coded space-time block signaling . . . . .	49
6.2	Space-time codes . . . . .	56
6.2.1	Space-time trellis codes . . . . .	58
6.2.2	Super-orthogonal space-time trellis codes . . . . .	63
6.2.3	Linear-dispersion codes . . . . .	65
Chapter 7. Conclusion and future work		69
Bibliography		72
VITA		

## LIST OF FIGURES

2.1	Tarokh's 4-state QPSK space-time trellis code . . . . .	14
2.2	2-state BPSK super-orthogonal space time code . . . . .	16
5.1	Concatenated channel code and space-time block code . . . . .	35
5.2	Convolutional Code, 2-Tx and 1-Rx antennas, $d = 6$ , Block by block i.i.d. Rayleigh fading . . . . .	37
5.3	One possible block pattern for the case $N = 5, d = 4, \ell = 2$ . . . . .	39
6.1	Convolutional code, block i.i.d. Rayleigh Fading, 2-Tx and 1-Rx antennas	50
6.2	Convolutional code, block i.i.d. Rayleigh Fading, 2-Tx and 2-Rx antennas	50
6.3	Convolutional code, 2-Tx and 1-Rx antennas, time correlated Rayleigh Fading, $F_d T_s = 0.1$ . . . . .	51
6.4	Turbo code, block i.i.d. Rayleigh Fading 2-Tx and 1-Rx antennas N=500	52
6.5	Turbo code, Quasi-static Rayleigh Fading 2-Tx and 1-Rx antennas, N=100 . . . . .	53
6.6	TCM, 2-Tx and 1-Rx antennas, block i.i.d. Rayleigh fading, BER . .	53
6.7	TCM, 2-Tx and 1-Rx antennas, block i.i.d. Rayleigh fading, FER . .	54
6.8	TCM, 2-Tx and 1-Rx antennas, quasi-static Rayleigh fading . . . . .	55
6.9	MTCM, 2-Tx and 1-Rx antennas, block i.i.d. Rayleigh Fading . . . . .	55
6.10	MTCM, 2-Tx and 1-Rx antennas, quasi-static Rayleigh Fading . . . . .	56
6.11	TCM, 2-Tx and 1-Rx antennas, block i.i.d. Rician fading $K = 5dB$ . .	57
6.12	PEP of a dominant codeword, STT code, 2-Tx, 2-Rx, quasi-static Rayleigh fading . . . . .	59
6.13	STT code, 2-Tx, 2-Rx, fast Rayleigh fading, $\rho_t = \rho_r = 0.7$ , FER . . .	60
6.14	STT code, 2-Tx, 2-Rx, fast Rayleigh fading, $\rho_t = \rho_r = 0.7$ , BER . . .	60
6.15	STT code, 2-Tx, 4-Rx, quasi-static Rayleigh fading, $\rho_t = \rho_r = 0.7$ . .	61
6.16	STT code, 2-Tx, 2-Rx, quasi-static Rayleigh fading . . . . .	62
6.17	STT code, 2-Tx, 4-Rx, temporally correlated Rayleigh fading, $f_d T_s =$ 0.01 . . . . .	63
6.18	SOSTT code, 2-Tx, 1-Rx, fast Rayleigh fading, $\rho_t = 0.7$ . . . . .	64
6.19	SOSTT code, 2-Tx, 4-Rx, quasi-static Rayleigh fading, $\rho_t = \rho_r = 0.7$ .	65

6.20	SOSTT code, 2-Tx, 4-Rx, temporally correlated Rayleigh fading, $f_d T_s = 0.01$ . . . . .	66
6.21	LD code, 2-Tx, 2-Rx, QPSK, Rayleigh fading . . . . .	67
6.22	LD code, 2-Tx, 2-Rx, 16QAM, Rayleigh fading . . . . .	68

## CHAPTER 1

### INTRODUCTION

#### 1.1 Wireless communications

The increasing demand for high data rates in wireless communications due to emerging new technologies makes wireless communications an exciting and challenging field. The spectrum or bandwidth available to the service provider is often limited and the allotment of new spectrum by the federal government is often slow in coming. Also, the power requirements are that devices should use as little power as possible to conserve battery life and keep the products small. Thus, the designers for wireless systems face a two-part challenge, increase data rates and improve performance while incurring little or no increase in bandwidth or power. The wireless channel is by its nature random and unpredictable, and in general channel error rates are poorer over a wireless channel than over a wired channel. A major problem in the wireless channel is that out-of-phase reception of multipaths causes deep attenuation in the received signal, known as fading. The distortion induced by the time-varying fading is caused by the superposition of delayed, reflected, scattered and diffracted signal components. Another problem of the wireless channel is variation over time, due to the movements of the mobile unit and objects in the environment. This results into severe attenuation of the signal, referred to as deep fade. This instantaneous decrease of the signal-to-noise ratio (SNR) results in error bursts which degrades the performance significantly.

In such fading environments, reliable communication is possible through the

use of diversity techniques in which the receiver is afforded multiple replicas of the transmitted signal under varying fading conditions. These techniques reduce the probability that all the replicas are simultaneously affected by a severe attenuation. Commonly used methods include:

- Frequency diversity, in which the signal is transmitted on multiple RF carriers;
- Temporal diversity, in which channel coding and interleaving are used to replicate and distribute the signal in time;
- Antenna/spatial diversity, in which multiple antennas are used at the transmitter and/or the receiver to provide multiple replicas of the signal with decorrelated fading characteristics.

Information theoretic investigations in the past few years [12, 13] have shown that very high capacity can be obtained by employing multiple antenna elements at both the transmitter and the receiver of a wireless system. These investigations have led to the development of a novel multiple transmit-receive architecture called Bell Labs Layered Space-Time Architecture (BLAST) [12], which provides transmission rates that are unattainable by traditional techniques. Another approach that uses multiple transmit antennas and (optionally) multiple receive antennas is Space-Time Coding (STC) [34]. First introduced in [34, 32] to provide high data rates and reliable communications over fading channels, this concept combines coding, modulation and spatial diversity into a two-dimensional coded modulation technique. Examples of space-time coding include space-time trellis codes, space-time block codes, super-orthogonal space-time codes and linear-dispersion (LD) codes. Space-time trellis codes provide full diversity and coding gain at the cost of a complex receiver. Space-time block codes provide full diversity and simple decoding, but no coding

gain. BLAST and STC make use of both the space (different antennas) and the time domain while encoding and decoding information symbols. Hence, the phrase space-time coded modulation can be generically applied to both techniques. We use the terms multiple-input multiple-output (MIMO) and space-time coding interchangeably in this thesis.

The analysis of MIMO systems usually consists of union bounds on bit and frame error probabilities, which in turn depend on pairwise error probability (PEP). PEP is defined as the probability of erroneously decoding codeword  $\hat{\mathbf{x}}$  when  $\mathbf{x}$  was transmitted. This kind of analysis makes it easier to compare two systems based on some criterion, and also provides insights into the working mechanism behind these codes. This analysis is also useful in developing design criteria.

Most of the existing work in this area assumes that the antenna elements at the transmitter and the receiver of the MIMO system are placed far enough (spatially) such that the effect of the channel at a particular antenna element is different from the effect at all other antenna elements. This implies independent or spatially uncorrelated fading. This holds true only if spacing between transmit antennas or receive antennas is of the order of several wavelengths. However, if antenna spacing is not enough, the fading channel from multiple antennas might be correlated, and the performance will be degraded. Similarly, some of the existing works assume quasi-static fading in which the channel characteristic remain constant over one frame period, while some others assume i.i.d. (fully interleaved) fading in which channel varies from one symbol to another independently. However, one may not be able to interleave codewords due to delays involved in interleaving. In that case, the channel will have temporal correlation. In this work, we analyze several space-time signaling schemes in presence of spatially and temporally correlated Rayleigh as well as Rician fading.

## 1.2 Literature review

Receive diversity existed as far back as 1960 [29]. However, receive diversity is not suitable for downlink in mobile communications, hence transmit diversity has attracted attention. Alamouti presented basic two transmit diversity scheme [1] and Tarokh et al. [32] extended it to general case, called orthogonal space-time block codes (OSTBC). OSTBC have full diversity ( $n_T \times n_R$ ), but have little or no coding gain. To provide both diversity and coding gain, one can choose a space-time code that has an in-built channel coding mechanism, for example space-time trellis codes, or one can choose a space-time block code concatenated with an outer channel code. Borran et al. [8] discuss design issues of concatenating channel codes with OSTBC. They show that design issues in maximizing diversity gain, and maximizing coding gain can be decoupled. Due to this simplicity, this structure has been accepted, e.g. in WCDMA standard. Gong and Ben Letaief [14] discuss design of concatenated trellis coded modulation (TCM) and OSTBC, and also show that this scheme outperforms space-time trellis codes with the same spectral efficiency, trellis complexity and signal constellation. Bauch and Hagenauer [4] give a new view of OSTBC over fading channel as an equivalent SISO channel. Using this equivalent channel model, they give analytical evaluation of error probability, without considering the effect of block fading (which is typically assumed for linear decoding of STBC). Uysal and Georghiades [37] give error bounds for MTCM-STBC under Rician Fading. However, interleaving does not appear in their analysis. Schulze [26] gives union bounds for channel codes and Alamouti signaling for temporally correlated and i.i.d. channel. But again, the block fading assumption is absent in his analysis. None of the above mentioned works discuss spatially correlated fading. Lai and Mandyam [21] simulate concatenated convolutional/turbo codes with two temporally and spatially correlated antennas in the framework of WCDMA, but do not provide any analysis.

Another class of space-time codes is trellis based space-time codes (e.g. space-time trellis codes [34], super-orthogonal space-time trellis codes [18] etc.). These codes incorporate coding and diversity into a single design. Much of the analysis of these systems concentrates on uncorrelated antennas, e.g., the analysis of space-time codes in i.i.d. fading in [28] and the analysis of super-orthogonal codes in [30]. In a few isolated cases, attempts have been made to explore the performance of MIMO systems when antennas are correlated. Damen, Abdi and Kaveh [11] study, via simulations, the effect of parameters such as angle spread and Rician factor on the performance of various space-time signaling and detection schemes. Bölcski and Paulraj [7] concentrate on the quasi-static channel and find Chernoff bounds that in the high-SNR regime link the diversity to the rank and eigenvalues of the correlation matrices. Their analysis yields expressions that are equivalent to, but different from, the ones we provide in this work in the special case of quasi-static channel. They also calculate the degradation of average pairwise error probability due to antenna correlation. Uysal and Georghiades [36] derive pairwise error probability expressions for transmit antenna correlation (with no receive correlation or temporal correlation).

### 1.3 Scope and outline of the thesis

In this work, our intent is to present an analysis that is general and comprehensive. We extend existing results as well as present new ones. We assume that the channel conditions are known exactly to the receiver, i.e. we have perfect channel state-information (CSI). We present the analysis in two parts. In the first part, we analyze concatenated channel codes and orthogonal space-time block codes [27]. This provides full diversity as well as coding gain. As the outer codes, we consider convolutional codes, turbo codes, TCM and MTCM. In the second part, we present generalized analysis for all space-time codes [17]. space-time codes, and

linear-dispersion codes. In particular,

1. We derive error bounds for the case of i.i.d. fading as well as spatially correlated or temporally correlated channels,
2. We include the effects of block fading in our analysis,
3. We give general analysis with respect to the number of transmit and receive antennas,
4. We analyze in the presence of fast fading and quasi-static fading in Rayleigh and Rician channels,

The organization of this thesis is as follows. Chapter 2 is a tutorial on the space-time signaling schemes analyzed. In Chapter 3 we present the analytical tools used throughout the research in deriving various bounds. Using these tools, we derive union bounds for bit and frame error probabilities of coded space-time block codes in Chapter 5. We develop bounding techniques and analyze the concatenated system under i.i.d. fading, spatially correlated fading, and spatio-temporally correlated fading. Chapter 4 gives analytical bounds for space-time trellis codes, super-orthogonal codes, and LD codes for spatially as well as temporally correlated and i.i.d. channels. In Chapter 6 we apply the derived PEPs to obtain bounds on frame and bit error rates of various codes. We also provide simulations to gauge the accuracy of the bounds and to demonstrate the effect of correlations.

## CHAPTER 2

### OVERVIEW OF SPACE-TIME SIGNALING

Schemes which use multiple transmit and receive antennas for communicating over a wireless channel are usually called Multiple-input multiple-output (MIMO) schemes. This chapter gives an introduction to MIMO systems or more specifically, space-time signaling; a technique used to transmit symbols from multiple antennas. The chapter is organized as follows. Section 2.1 gives a brief description of channel models which are used to characterize the performance of MIMO schemes. Section 2.2 explains the concept of diversity. Section 2.2.1 introduces transmit diversity and provides a detailed description of the basic features of Space-Time Block Codes. Section 2.2.2 gives a description of space-time trellis codes. Sections 2.2.3 and 2.2.4 explain two new technologies super-orthogonal space time codes and LD codes respectively. In Section 2.3 we summarize and point out some references for further reading.

#### 2.1 Multiple-input multiple-output (MIMO) channels

To effectively evaluate the performance of a MIMO transmission scheme, models which account for all the major effects of wireless channel on various signals are required. The most commonly used channel model for MIMO systems is quasi-static flat Rayleigh fading at all antenna elements. This was employed in [12, 1, 34, 32, 33] where novel signal processing schemes for MIMO systems were introduced. The simplicity of this channel model made the performance analysis of these schemes less

complicated, allowing the authors to place more emphasis on introducing the transmit and receive signal processing algorithms. Fundamental Information theoretic results on capacity of MIMO channels [13] and transmit diversity techniques also employ a similar fading channel model. The basic assumptions behind the quasi-static flat Rayleigh fading channel are

- A large number of scatterers are present in the wireless channel so that the signal at any receive antenna of the MIMO system is the sum of several multipath components. In this case the distribution of the received signal at each antenna will be complex Gaussian. The amplitude of such complex Gaussian distributed signals is Rayleigh distributed.
- The channel delay spread, which is a measure of the difference in the time of arrival of various multipath components at the receiver antenna, is less than the symbol rate. This assumption guarantees flat fading.
- The channel characteristics remain constant at least for the period of transmission of an entire frame. This assumption accounts for quasi-static fading.

Using all these assumptions, the quasi-static flat Rayleigh fading MIMO channel for a system with  $n_T$  transmit and  $n_R$  receive antennas can be represented as

$$\mathbf{H} = \begin{bmatrix} h_{11} & h_{12} & \dots & h_{1n_T} \\ h_{21} & h_{22} & \dots & h_{2n_T} \\ \vdots & \vdots & \ddots & \vdots \\ h_{n_R1} & h_{n_R2} & \dots & h_{n_Rn_T} \end{bmatrix}$$

where  $h_{ij}$  is the path gain between receive antennas  $i$  and transmit antenna  $j$ . The path gains are usually modeled as zero mean complex Gaussian random variables with variance 0.5 per real dimension.

## 2.2 Diversity techniques

Let us consider a system with BPSK modulation transmitting under fading channel with Gaussian noise. The complex channel coefficient is denoted by  $h$  and its magnitude is denoted by  $\alpha$ . It is assumed that the phase of fading coefficient is perfectly known at the receiver (i.e. coherent detection). The conditional error rate of BPSK as a function of channel coefficient over frequency non-selective, slowly fading channel is given by [25],

$$P_b(\alpha) = Q(\sqrt{2\gamma}) \quad (2.1)$$

where  $\gamma = \frac{\alpha^2 E_b}{N_0}$  is the received SNR. To find unconditional error rate, we must integrate over all possible values of fading coefficient. Assuming Rayleigh fading, this integration is

$$P_b = \frac{1}{2} \left( 1 - \sqrt{\frac{\bar{\gamma}}{1 + \bar{\gamma}}} \right) \quad (2.2)$$

where  $\bar{\gamma} = \frac{E_b}{N_0} \mathcal{E}(\alpha^2)$  is the average SNR. In high SNR region this error probability can be approximated as

$$P_b \approx \frac{1}{4\bar{\gamma}}$$

Note that the error rate decreases inversely with SNR. Compare this to the error rate of BPSK in non-fading (AWGN) channel [25],

$$P_b = Q\left(\sqrt{\frac{2E_b}{N_0}}\right) \quad (2.3)$$

which decreases exponentially with SNR. This means that on a fading channel the transmitter should transmit with more power to achieve a low probability of error.

As mentioned in the first chapter, diversity techniques are very effective against fading channel. If we can supply several replicas of the transmitted signal to the receiver, it is unlikely that all of them will undergo deep fade simultaneously. If we have supplied  $L$  independently faded replicas of transmitted signal to the receiver,

and  $p$  is the probability that any one replica will undergo deep fading,  $p^L$  is the probability that all the  $L$  replicas will undergo deep fading. There are several types of diversity – frequency diversity, polarization diversity, time diversity, and spatial diversity. In this thesis, we are only interested in spatial (antenna) diversity.

Traditionally, there is only single transmit antenna and multiple receive antenna. This technique is referred to as receive diversity. The receiver can use one of three techniques to improve the quality of received signal:

1. Selection: select the received signal with largest received power.
2. Switching: choose alternate antennas if the received power falls below a threshold level.
3. Maximal Ratio Combining (MRC): linearly combine a weighted replica of all received signals.

In the method of MRC, it is assumed that the receiver has perfect channel side-information. If the transmitted signal at time  $t$  is  $s(t)$ , the received signal at receiver  $i$  is given by,

$$r_i(t) = s(t)h_i(t) + n_i(t)$$

where  $n_i(t)$  is complex noise variable. Assuming that this noise is Gaussian, the receiver combining scheme is

$$\tilde{r}(t) = \sum_{i=1}^{n_R} h_i^* r_i(t) = s(t) \sum_i^{n_R} |h_i|^2 + n'(t)$$

This detected symbol is then passed through a maximum-likelihood detector to produce the estimate of transmitted signal  $\tilde{s}(t)$ . MRC provides full diversity, but due to channel estimation the complexity is high.

### 2.2.1 Transmit diversity and space-time block codes

The receive diversity scheme is not suitable for the downlink, as it is difficult and inconvenient to install multiple antennas on handsets. The multiple antenna burden is preferably placed at the base station. This is called transmit diversity. Transmit diversity has gained a lot of attraction and research in last five years [1, 32]. Unlike in receive diversity, in transmit diversity it is not possible to transmit the same signal from all antennas. If same signal is transmitted from all the antennas, at the receiver the copies of this signal add incoherently, and no diversity gain can be achieved. Thus in order for transmit diversity to work, one must find a transmission scheme where replicas of the signal combine coherently at the receiver.

One of the simplest and most attractive transmit diversity schemes were proposed by Alamouti,

$$\mathcal{G}_2 = \begin{pmatrix} s_1 & s_2 \\ -s_2^* & s_1^* \end{pmatrix} \quad (2.4)$$

where the rows denote time instances and columns denote transmit antennas. Thus, at time  $t = 1$ ,  $s_1$  and  $s_2$  will be transmitted from antennas 1 and 2 respectively, and at time  $t = 2$ ,  $-s_2^*$  and  $s_1^*$  will be transmitted from antennas 1 and 2 respectively. One can see that two symbols are transmitted over two time intervals. Hence the code is full rate. Assuming a single receiver, let  $h_1$  and  $h_2$  denote the channel coefficients for transmit antenna 1 and 2 respectively. The fading coefficients are assumed to be constant over  $n_T = 2$  consecutive time slots.

$$h_1 = h_1(T = 1) = h_1(T = 2)$$

$$h_2 = h_2(T = 1) = h_2(T = 2)$$

Hence the received signal is,

$$y_1 = h_1 x_1 + h_2 x_2 + n_1 \quad (2.5)$$

$$y_2 = -h_1 x_2^* + h_2 x_1^* + n_2 \quad (2.6)$$

With perfect SI, this can be maximum-likelihood (ML) decoded as,

$$\tilde{x}_1 = h_1^* y_1 + h_2 y_2^* = (|h_1|^2 + |h_2|^2)x_1 + \tilde{n}_1 \quad (2.7)$$

$$\tilde{x}_2 = h_2^* y_1 - h_1 y_2^* = (|h_1|^2 + |h_2|^2)x_2 + \tilde{n}_2 \quad (2.8)$$

We observe from the above expression that by using two transmit and one receive antenna, the transmitted signals are effectively multiplied by  $|h_1|^2 + |h_2|^2$ . Hence, if one of the paths is in deep fade, the other may still represent the signal with reliability. In fact, the use of orthogonal STBC changes the probability distribution of the channel to distribution with lower variance. It can also be observed that OSTBC in MIMO channels can be represented as equivalent SISO channel, which discuss in detail in Chapter 5.

Tarokh et al. [32] extended the Alamouti's 2-transmit diversity scheme to more than two antennas. This new generalized space-time signaling scheme is known as space-time block codes (STBC). Space-time block codes derive their name from the fact that the encoding is done in both space and time, and their encoder is defined simply by a matrix. A space-time block code is defined by the relationship between the  $k$ -tuple input signal  $\mathbf{x}$  and the set of signals to be transmitted from  $n_T$  antenna over  $p$  time periods. Such a relation is given by  $p \times n_T$  transmission matrix

$$\mathcal{G} = \begin{bmatrix} s_{11} & s_{12} & \dots & s_{1n_T} \\ s_{21} & s_{22} & \dots & s_{2n_T} \\ \vdots & \vdots & \ddots & \vdots \\ s_{p1} & s_{p2} & \dots & s_{pn_T} \end{bmatrix} \quad (2.9)$$

where  $s_{ij}$  are functions of  $k$ -tuple input sequence  $x_1, x_2, \dots, x_k$  and their complex conjugates. At time slot  $i$ ,  $s_{ij}$  is transmitted from antenna  $j$ . Since  $k$  information bits are transmitted over  $p$  time interval, the rate of the code is defined as  $R = \frac{k}{p}$ . At the receiver we can use arbitrary number of receive antennas. The design does not depend on the number of receive antennas  $n_R$ .

If  $\mathcal{G}\mathcal{G}^H = \alpha\mathbf{I}$ , where  $\alpha = \sum_{n=1}^{n_T} |s_n|^2$  and  $\mathbf{I}$  is the identity matrix, the code is called orthogonal STBC. The orthogonal STBC assumes that the channel coefficients are constant over a period of  $n_T$  symbols, i.e.

$$h_{ij}(t) = h_{ij} \quad t = 1, 2, \dots, n_T \quad (2.10)$$

This block fading assumption is required for simple linear decoding of OSTBC. OSTBC also assumes that the channel is frequency non-selective. If the channel is frequency selective, one can use orthogonal frequency division multiplexing (OFDM) to split the input bit stream into large number of low-rate streams transmitted over flat fading channels. In our work, we only consider frequency non-selective channels.

At the receiver, the  $n_R$  receive antennas use maximum likelihood (ML) decoding. In orthogonal STBC the ML decoding is equivalent to maximum ratio combining (MRC). Assuming perfect channel side-information (SI), the decoder at antenna  $j$  maximizes

$$\sum_{t=1}^p \sum_{j=1}^{n_R} \left| r_t^j - \sum_{i=1}^{n_T} h_{ji} x_t^i \right|^2 \quad (2.11)$$

Since the block coding requires only linear processing at the receiver, the decoding can be done efficiently and quickly. Space-time block codes can be constructed for any type of signal constellation and provide full diversity. However, only real constellations such as Pulse Amplitude (PAM) can give full rate for any number of antennas. For complex constellations such as Phase Shift Keying (PSK), full rate STBC exist only for  $n_T = 2$ .

### 2.2.2 Space-time trellis codes

Space-time trellis codes (STTC), originally proposed by Tarokh et al. [34], incorporate jointly designed channel coding, modulation, transmit diversity and optional receive diversity.

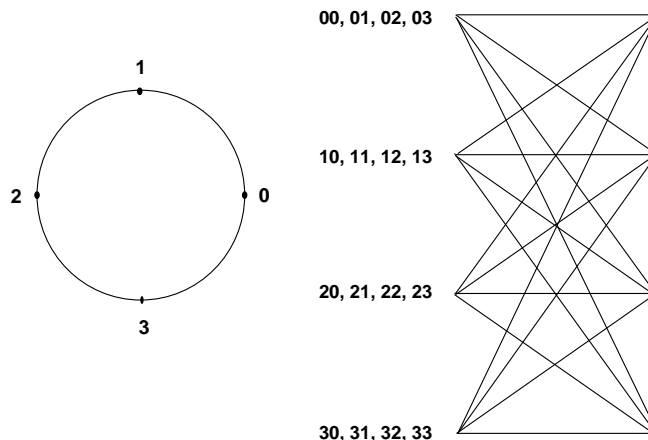


Figure 2.1. Tarokh's 4-state QPSK space-time trellis code

As the name suggests, the structure of space-time trellis code is given by a trellis. A trellis for 4-state QPSK STTC with two transmit antennas [34] is given in Figure 2.1. Here the first QPSK symbol is transmitted from first antenna and the second QPSK symbol is transmitted from second antenna, at time instance  $t$ . Thus, at each time instance one information symbol is transmitted, and the rate is 1.

The  $n_R \times 1$  received signal is given by

$$\mathbf{y}_t = \mathbf{H}_t \mathbf{s}_t + \mathbf{n}_t \quad (2.12)$$

Where  $\mathbf{H} = \{h_{ji}\}$   $i = 1, \dots, n_T$   $j = 1, \dots, n_R$  is the channel matrix and  $\mathbf{s} = [s_1, \dots, s_{n_T}]^T$  is the transmitted vector at time instance  $t$ . A codeword  $\mathbf{c}$  is given by

$$\mathbf{c} = \begin{bmatrix} c_1(1) & c_1(2) & \dots & c_1(N) \\ c_2(1) & c_2(2) & \dots & c_2(N) \\ \vdots & \vdots & \ddots & \vdots \\ c_{n_T}(1) & c_{n_T}(2) & \dots & c_{n_T}(N) \end{bmatrix}$$

An error event is given by  $\mathbf{B}(\mathbf{c}, \mathbf{e}) = \mathbf{c} - \mathbf{e}$ .

The probability of erroneously decoding  $\mathbf{e}$  when  $\mathbf{c}$  was transmitted, called pairwise error probability (PEP) is given by,

$$P(c, e) \leq \left( \prod_{i=1}^r \lambda_i \right)^{-n_R} \left( \frac{E_s}{4N_0} \right)^{-rn_R} \quad (2.13)$$

where  $r$  is the rank of  $\mathbf{A}(\mathbf{c}, \mathbf{e}) = \mathbf{B}(\mathbf{c}, \mathbf{e})\mathbf{B}^H(\mathbf{c}, \mathbf{e})$  and  $\lambda$  are the nonzero eigenvalues of  $\mathbf{A}(\mathbf{c}, \mathbf{e})$ . From this equation, the design criteria can be given as

1. Rank criterion: To achieve maximum possible diversity,  $n_T \times n_R$ , matrix  $\mathbf{A}(\mathbf{c}, \mathbf{e})$  should be full rank for all the codewords.
2. Determinant criterion: To maximize the coding gain, minimum determinant of  $\mathbf{A}(\mathbf{c}, \mathbf{e})$  should be maximized over all codewords.

### 2.2.3 Super-orthogonal space-time codes

Space-time trellis codes provide full diversity and full rate. There exist some design criteria that must be satisfied to obtain full diversity. However, there is no systematic design method available and one has to do a computer search to obtain best possible codes. Also, it is not clear how to improve performance of such codes. sOSTBC provide full rate and full diversity with a very simple design, but do not provide any coding gain. To achieve additional coding gain [8, 14] combine space-time block codes with trellis codes. However, this reduces the rate of the resultant code.

To solve this problem, Jafarkhani and Seshadri [18] proposed a new coding scheme which combines STBC with trellis codes and yet guarantees full rate. They also provide systematic design criteria similar to the design criteria of TCM. The authors [18] of recognize that a space-time block code does not use all the possible transmission matrices. For example Alamouti's scheme is defined by the following transmission matrix:

$$\mathcal{C}(s_1, s_2) = \begin{pmatrix} s_1 & s_2 \\ -s_2^* & s_1^* \end{pmatrix}$$

However, all possible  $2 \times 2$  orthogonal transmission matrices are:

$$\begin{pmatrix} s_1 & s_2 \\ -s_2^* & s_1^* \end{pmatrix} \begin{pmatrix} -s_1 & s_2 \\ s_2^* & s_1^* \end{pmatrix} \begin{pmatrix} s_1 & -s_2 \\ s_2^* & s_1^* \end{pmatrix} \begin{pmatrix} s_1 & s_2 \\ s_2^* & -s_1^* \end{pmatrix}$$

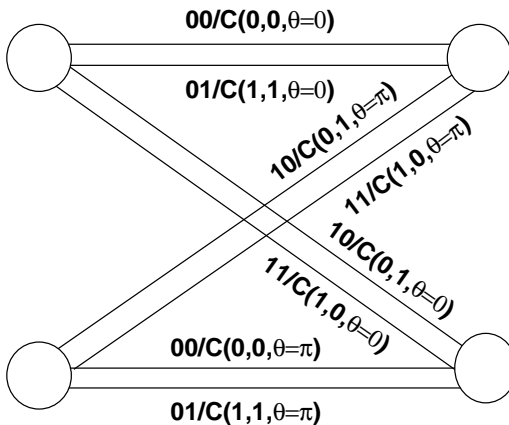


Figure 2.2. 2-state BPSK super-orthogonal space time code

$$\begin{pmatrix} -s_1 & -s_2 \\ s_2^* & -s_1^* \end{pmatrix} \begin{pmatrix} -s_1 & s_2 \\ -s_2^* & -s_1^* \end{pmatrix} \begin{pmatrix} s_1 & -s_2 \\ -s_2^* & -s_1^* \end{pmatrix} \begin{pmatrix} -s_1 & -s_2 \\ -s_2^* & s_1^* \end{pmatrix}$$

Super-orthogonal space-time codes (SOSTC) are essentially space-time trellis codes transmitting space-time block (STB) codewords in each trellis section. The set of available STB codewords are extended via rotations, while maintaining the orthogonality of the codewords. Thus, all the eight transmission matrices are used in case of 2 transmit antenna SOSTC. Finally, a set partitioning is performed for efficient labeling of the trellis. For example, in the case of Alamouti signaling, there are  $n_T = 2$  time intervals per trellis section and the set of codewords are represented by

$$\mathcal{C}(s_1, s_2, \theta) = \begin{pmatrix} s_1 e^{j\theta} & -s_2^* e^{j\theta} \\ s_2 & s_1^* \end{pmatrix} \quad (2.14)$$

with  $\theta = 0, \frac{\pi}{2}$ . The resulting code has a systematic design procedure, and shows better performance compared to the reported STT codes [18]. A two-state BPSK super-orthogonal code is shown in Figure 2.2. The labels on the branches show output of the trellis. The output of the trellis is used with Equation 2.14, and then mapped to the two transmit antennas.

### 2.2.4 Linear-dispersion codes

The space-time coding systems we have explained so far concentrate on improving error performance and providing diversity. However, they do so at rates below the capacity of MIMO system. Also, these systems become either too complex (e.g. STTC) or their performance degrades considerably at high data rates (e.g. STBC). There are other space-time signaling schemes that concentrate on increasing the rate of the system, while providing little or no improvement in error performance. For example, Vertical Bell Labs Layered Space-Time Architecture (V-BLAST) supports a high data rate. In V-BLAST, every transmit antenna transmits its own sub-stream of data. V-BLAST suffers from two problems: 1) It requires more receive antennas than transmit antennas. This might not be possible in cellular systems, where the number of antennas at base station is typically more than number of antennas at mobile handset. 2) It does not provide any diversity gain. To achieve high data rates as well as diversity, Hassibi and Hochwald [16] propose a new scheme in which transmitter sends sub-streams of data in linear combinations over space and time. This new scheme allows any number of transmit and receive antennas, provide diversity gain, and maximize the mutual information between transmitter and receiver. This new codes, called Linear dispersion (LD) codes have codeword matrices  $\mathbf{X}_{n_T \times T}$  such that

$$\mathbf{X} = \mathbf{X}(x_1 = \alpha_1 + j \beta_1, \dots, x_Q = \alpha_Q + j \beta_Q) = \sum_{q=1}^Q (\alpha_q A_q + j \beta_q B_q) \quad (2.15)$$

where  $x_q = \alpha_q + j \beta_q$  is a signal chosen from an M-PSK or M-QAM modulation, and  $A_q$  and  $B_q$  are complex spreading matrices with size  $n_T \times T$  where  $T$  is the time-span of each codeword. Each entry of the codeword  $\mathbf{X}$  is a linear combination of all  $x_q$ 's. There are  $Q$  signals to be transmitted in  $T$  consecutive time instances and correspondingly  $Q$  spreading matrices  $A_q$  and  $B_q$ . The code has  $M^Q$  codewords

where  $M$  is the number of signals in the constellation. It is assumed that the channel matrix is known to the receiver, and the parameters  $Q$ ,  $A_q$ , and  $B_q$  are chosen to maximize the mutual information that the LD code can attain [16]. There exist efficient algorithms for near-ML and sub-optimal successive nulling and cancelling decoders for LD codes.

For example, a LD code with  $n_T = 2$ ,  $n_R = 2$ ,  $T = 2$ , and  $Q = n_T \times T = 4$  is given by the following matrices [16],

$$\begin{aligned} A_1 = B_1 &= \frac{1}{\sqrt{2}} \begin{pmatrix} 1 & 0 \\ 0 & 1 \end{pmatrix}, & A_2 = B_2 &= \frac{1}{\sqrt{2}} \begin{pmatrix} 0 & 1 \\ 1 & 0 \end{pmatrix} \\ A_3 = B_3 &= \frac{1}{\sqrt{2}} \begin{pmatrix} 1 & 0 \\ 0 & -1 \end{pmatrix}, & A_4 = B_4 &= \frac{1}{\sqrt{2}} \begin{pmatrix} 0 & 1 \\ -1 & 0 \end{pmatrix} \end{aligned}$$

### 2.3 Further reading

In this chapter, we give an overview of the current state of technology in space-time coding. For further reading, we point out a few interesting and informative references here. Various models for fading channels are given in [31]. The book [29] provides excellent material for fading channels and diversity techniques, especially for receive diversity. A good tutorial on space-time block codes and space-time trellis codes can be found in [15]. An in depth study of MIMO systems as well as space-time block codes can be found in [22].

## CHAPTER 3

### ANALYTICAL TOOLS

In this chapter, we explain the analytical tools used to derive the pairwise error probabilities in later chapters. Of particular interest is the alternative expression for Q-function [29] explained in Section 3.3.

#### 3.1 Spatially correlated channel

If the antenna elements in either the transmitter or the receiver are not far enough apart, the fading coefficients  $h_{ij}$  will be correlated. We do not assume any specific structure for the correlation of fading coefficients, and the analysis is general in that sense. We do assume that the correlation structure is stationary (time-invariant).

The correlations can be modeled using a virtual linear system operating on an innovations channel  $\tilde{\mathbf{H}}$ , which has i.i.d. components. The most general form of such a correlation model is constructed using the vectorizing operator  $\text{vec}(\cdot)$  as follows.

**Lemma 1** *Consider a random matrix  $\tilde{\mathbf{H}}$  with i.i.d. entries, and two deterministic, positive semi definite matrices  $\mathbf{A}$  and  $\mathbf{B}$  of appropriate size, and assume  $\mathbf{H} = \mathbf{A}^{1/2} \tilde{\mathbf{H}} \mathbf{B}^{1/2}$ . Then  $\mathbf{H}$  can be equivalently represented thus:*

$$\text{vec}(\mathbf{H}) = \mathbf{R}^{1/2} \text{vec}(\tilde{\mathbf{H}}) \quad , \quad (3.1)$$

where  $\text{vec}(\cdot)$  is the vectorizing operator and  $\mathbf{R} = \mathcal{E}[\text{vec}(\mathbf{H})\text{vec}(\mathbf{H})^H] = \mathbf{B} \otimes \mathbf{A}$ , the Kronecker product of  $\mathbf{B}$  and  $\mathbf{A}$ .

**Proof:** Easily follows via the identities:

$$\text{vec}(\mathbf{AXB}) = (\mathbf{B}^T \otimes \mathbf{A})\text{vec}(\mathbf{X}) , \quad (3.2)$$

$$(\mathbf{A} \otimes \mathbf{B})^T = \mathbf{A}^T \otimes \mathbf{B}^T , \quad (3.3)$$

$$(\mathbf{A} \otimes \mathbf{B})(\mathbf{C} \otimes \mathbf{D}) = \mathbf{AC} \otimes \mathbf{BD} . \quad (3.4)$$

$$\begin{aligned} \text{vec}(\mathbf{H}) &= \text{vec}(\mathbf{A}^{1/2}\tilde{\mathbf{H}}\mathbf{B}^{1/2}) \\ &= (\mathbf{B}^{H/2} \otimes \mathbf{A}^{1/2})\text{vec}(\tilde{\mathbf{H}}) \end{aligned} \quad (3.5)$$

$$\begin{aligned} \mathbf{R} &= \mathcal{E}[\text{vec}(\mathbf{H})\text{vec}(\mathbf{H})^H] \\ &= \mathcal{E}[(\mathbf{B}^{H/2} \otimes \mathbf{A}^{1/2})\text{vec}(\tilde{\mathbf{H}})\text{vec}(\tilde{\mathbf{H}})^H(\mathbf{B}^{H/2} \otimes \mathbf{A}^{1/2})^H] \\ &= (\mathbf{B}^{H/2} \otimes \mathbf{A}^{1/2})(\mathbf{B}^{H/2} \otimes \mathbf{A}^{1/2})^H \\ &= (\mathbf{B}^{H/2} \otimes \mathbf{A}^{1/2})(\mathbf{B}^{1/2} \otimes \mathbf{A}^{H/2}) \\ &= \mathbf{B} \otimes \mathbf{A} \end{aligned} \quad (3.6)$$

□

This is closely related to an existing correlation model [9] where  $\mathbf{A}$  and  $\mathbf{B}$  represent the correlation matrices at the transmitter and receiver side, respectively. In other words,

$$\mathbf{H} = \mathbf{R}_{\text{Tx}}^{1/2} \tilde{\mathbf{H}} \mathbf{R}_{\text{Rx}}^{1/2} . \quad (3.7)$$

However, for our purposes, the following unitary transformation is more useful

$$\text{vec}(\mathbf{H}) = \mathbf{R}_s^{1/2}\text{vec}(\tilde{\mathbf{H}}) = \mathbf{U}\Lambda^{1/2}\text{vec}(\tilde{\mathbf{H}}) , \quad (3.8)$$

where  $\mathbf{R}_s = \mathbf{U}\Lambda\mathbf{U}^H$ . For future reference, it is useful to remember  $\Lambda = \Lambda_{\text{Tx}} \otimes \Lambda_{\text{Rx}}$ .

### 3.2 Union bounds on frame and bit error probability

For a given  $(N, K)$  code  $\mathcal{C}$  (where  $N$  is the codeword length and  $K$  is the number of information bits per codeword) the PEP can be used to calculate union

bounds on bit error probability

$$P_b \leq \frac{1}{K} \sum_{\mathbf{X} \in \mathcal{C}} P(\mathbf{X}) \sum_{\hat{\mathbf{X}} \neq \mathbf{X}} w P(\mathbf{X} \rightarrow \hat{\mathbf{X}}) \quad , \quad (3.9)$$

where  $w$  is the number of differing information bits between  $\mathbf{X}$  and  $\hat{\mathbf{X}}$ , and frame error probability,

$$P_e \leq \sum_{\mathbf{X} \in \mathcal{C}} P(\mathbf{X}) \sum_{\hat{\mathbf{X}} \neq \mathbf{X}} P(\mathbf{X} \rightarrow \hat{\mathbf{X}}) \quad . \quad (3.10)$$

However, this requires knowledge of all the codewords, and all the PEPs. This might be computationally cumbersome. If the code is linear, or it possesses a special property called uniform error probability (UEP) [29], there exists an easier approach – weight distribution of the code. The input output weight enumerating function (IOWEF) gives the multiplicities of codewords with input weight  $w$  and output weight  $d$ ,

$$A(W, D) = \sum_{w,d} A_{w,d} W^w D^d \quad (3.11)$$

The frame error rate is given by,

$$P_e \leq \sum_{w=0}^K \sum_{d=0}^N A_{w,d} P(d) \quad (3.12)$$

and the bit error rate is given by,

$$P_b \leq \sum_{w=0}^K \sum_{d=0}^N \frac{w}{K} A_{w,d} P(d) \quad (3.13)$$

For example, let us consider a systematic (7, 4) Hamming code with generator matrix

$$\mathbf{G}(D) = \begin{bmatrix} 1 & 0 & 0 & 0 & 1 & 0 & 1 \\ 0 & 1 & 0 & 0 & 1 & 1 & 1 \\ 0 & 0 & 1 & 0 & 1 & 1 & 0 \\ 0 & 0 & 0 & 1 & 0 & 1 & 1 \end{bmatrix}$$

The WEF of the code is

$$A(X) = 1 + 7X^3 + 7X^4 + X^7$$

and the IOWEF of the code is

$$A(W, X) = 1 + 3WX^3 + WX^4 + 3W^2X^3 + 3W^2X^4 + W^3X^3 + 3W^3X^4 + W^4X^7$$

The IOWEF shows that there are three codewords with input weight one and output weight three, one codeword with input weight one and output weight four, and so on.

In case of multilevel modulation,  $d$  is a vector,  $\mathbf{d} = (v_0, \dots, v_{2^m-1})$ , where  $v_i$  is the number of times symbol  $i$  appears in the codeword.  $P(d)$  is the probability of mistakenly decoding codeword with weight  $d$ , assuming all zero codeword was transmitted. To calculate bit and frame error probabilities we need to obtain corresponding PEPs  $P(d)$ , to which the remainder of this thesis is dedicated.

### 3.3 Alternative expression for Q function

For a given channel code  $\mathcal{C}$ , the probability of decoding  $\mathbf{e}$  when  $\mathbf{c}$  was transmitted, given the channel realization is,

$$P(\mathbf{c} \rightarrow \mathbf{e} | \gamma) = Q(\sqrt{\gamma}) \quad (3.14)$$

where  $\gamma = \frac{d^2(\mathbf{c}, \mathbf{e})E_s}{2N_0}$ , and  $d(\mathbf{c}, \mathbf{e})$  is the Euclidean distance between codewords  $\mathbf{c}$  and  $\mathbf{e}$ .

Traditionally, the PEP is given by Chernoff bound on Q-function. However, there is an exact yet simple alternative expression for Q-function due to Simon and Alouini.

$$Q(x) = \frac{1}{\pi} \int_0^{\pi/2} \exp\left(\frac{-x^2}{2 \sin^2 \theta}\right) d\theta \quad (3.15)$$

Using this expression, and averaging over all channel realizations, one can write the PEP as,

$$P(\mathbf{c} \rightarrow \mathbf{e}) = \frac{1}{\pi} \int_0^{\pi/2} \int_0^\infty \exp\left(-\frac{\gamma}{\sin^2 \theta}\right) p_\gamma(\gamma) d\gamma d\theta$$

We recognize the inner integral as the moment generating function (MGF) of  $\gamma$ ,  $\Phi(s) = \mathcal{E}[e^{-s\gamma}]$ , evaluated at  $s = -1/\sin^2\theta$ . Hence the PEP is given by,

$$P(\mathbf{c}, \mathbf{e}) = \frac{1}{\pi} \int_0^{\pi/2} \Phi_\gamma \left( -\frac{1}{\sin^2\theta} \right) d\theta \quad (3.16)$$

In the later chapters we derive the pairwise error probabilities for different codes in different channels. The Equations 3.10 and 3.12, along with the PEPs derived in later chapters, give very tight bounds for fast fading. However, in slow fading, the resulting upper bounds are very loose because there is no dominant error events. This has been observed widely in literature [28, 30, 24, 36]. Under these circumstances, to obtain tighter bounds, one can use either only a few error events in Equation 3.10, or use the method of limit before averaging. Limit before averaging method limits the conditional union bound on frame error probability before averaging over fading channel,

$$P_e \leq \int_\gamma \min(1, \sum_{\mathbf{X} \in \mathcal{C}} P(\mathbf{X}) \sum_{\hat{\mathbf{X}} \neq \mathbf{X}} P(\mathbf{X} \rightarrow \hat{\mathbf{X}})) f(\gamma) d\gamma \quad (3.17)$$

and bit error probability,

$$P_b \leq \int_\gamma \min(0.5, \sum_{\mathbf{X} \in \mathcal{C}} P(\mathbf{X}) \sum_{\hat{\mathbf{X}} \neq \mathbf{X}} \frac{w}{K} P(\mathbf{X} \rightarrow \hat{\mathbf{X}})) f(\gamma) d\gamma \quad (3.18)$$

Note that even with limit before averaging the bounds are 2-3 dB loose compared to simulation in quasi-static channel. This difference is usually reduced in higher diversity systems. For example compare figures 6.15 and 6.16. The bounds are looser in Figure 6.16 because there are only two receive antennas as compared to four receive antennas in Figure 6.16.

## CHAPTER 4

### ANALYSIS OF SPACE-TIME CODES

In this chapter we provide an analysis that is applicable to all space-time codes. To this end, we use the tools described in Chapter 3 to build analytical expressions for pairwise error probability.

#### 4.1 System model

We consider a MIMO system with  $n_T$  transmit and  $n_R$  receive antennas. The binary data is encoded and modulated by a space-time trellis encoder. Let  $\mathbf{x}_n = [x_1^{(n)}, \dots, x_{n_T}^{(n)}]^T$  denote the transmitted signal vector in the  $n$ -th time interval. Let  $\mathbf{H}_n = \{h_{ji}^{(n)}\}$  be the  $n_R \times n_T$  channel matrix at time  $n$ , where each entry  $h_{ji}$  is the channel gain between transmit antenna  $i$  and receive antenna  $j$ . The channel gains are assumed to be circularly symmetric complex Gaussian random variables, so their magnitude exhibits a Rayleigh distribution. The received signal vector at time  $n$  is given by

$$\mathbf{r}_n = \mathbf{H}_n \mathbf{x}_n + \mathbf{z}_n \quad , \quad (4.1)$$

where  $\mathbf{z}$  is a  $n_R \times 1$  independent and identically distributed (i.i.d.) zero-mean Gaussian noise vector. We assume that the receiver has perfect knowledge of the channel matrix and performs coherent detection. The maximum likelihood (ML) metric is given by,

$$m(\mathbf{r}, \mathbf{x}) = \sum_{n=1}^N \|\mathbf{r}_n - \mathbf{H}_n \mathbf{x}_n\|^2 \quad .$$

where  $N$  is the total frame (codeword) length,  $\mathbf{r}$  is the received signal in this period, and  $\mathbf{x}$  is a given codeword in the same period.

Using techniques made popular by the work of Simon and Alouini [29], we first calculate the conditional PEP and then integrate over channel gain coefficients. An error occurs when the noise random variable  $\mathbf{z}$  takes values larger than  $\|\mathbf{H}(\mathbf{x} - \hat{\mathbf{x}})\|$ . Denoting the codeword differences by  $\mathbf{\Delta}_n = \mathbf{x}_n - \hat{\mathbf{x}}_n$ , the PEP for a given channel realization is

$$P(\mathbf{x} \rightarrow \hat{\mathbf{x}}|\mathbf{H}) = Q \left( \sqrt{\frac{E_s}{2N_0} \sum_{n=1}^N \|\mathbf{H}_n \mathbf{\Delta}_n\|^2} \right) . \quad (4.2)$$

Now use the alternative integral expression of Q-function [29]

$$Q(x) = \frac{1}{\pi} \int_0^{\pi/2} \exp \left( -\frac{x^2}{2 \sin^2 \theta} \right) d\theta$$

and subsequently integrate over the randomness of the channel coefficients to obtain the unconditional PEP.

$$P(\mathbf{x} \rightarrow \hat{\mathbf{x}}|\mathbf{H}) = \frac{1}{\pi} \int_0^{\pi/2} \exp \left( -\frac{E_s}{4N_0 \sin^2 \theta} \sum_{n=1}^N \|\mathbf{H}_n \mathbf{\Delta}_n\|^2 \right) d\theta , \quad (4.3)$$

$$P(\mathbf{x} \rightarrow \hat{\mathbf{x}}) = \frac{1}{\pi} \int_0^{\frac{\pi}{2}} \Phi \left( -\frac{E_s}{4N_0 \sin^2 \theta} \right) d\theta , \quad (4.4)$$

where  $\Phi(\cdot)$  is the moment generating function of the random variable  $\sum_{n=1}^N \|\mathbf{H}_n \mathbf{\Delta}_n\|^2$ .

Whenever channel coefficients are spatially and temporally independent, the overall moment generating function can be decomposed into a product of marginal MGF's, thus the calculation of the above integral is simplified. In the presence of spatial or temporal correlation, however, this product decomposition does not exist and thus complications arise. This section is mainly devoted to providing analytical tools for the calculation of PEP under correlated channel conditions.

We first consider spatially correlated antennas. We use the spatially correlated channel model from Chapter 3. For easy reference, we state the result once again.  $\mathbf{H}$  is  $n_R \times n_T$  channel matrix. Transmit side correlation is  $\mathbf{R}_{\text{Tx}}$  and receive side

correlation is  $\mathbf{R}_{\text{Rx}}$ . Denoting an innovations channel with i.i.d. components as  $\tilde{\mathbf{H}}$ , the correlated channel can be represented as,

$$\mathbf{H} = \mathbf{R}_{\text{Rx}}^{1/2} \tilde{\mathbf{H}} \mathbf{R}_{\text{Tx}}^{1/2}$$

## 4.2 Quasi-static fading with spatial correlation

In quasi-static fading channel the matrix channel is assumed to be constant over the duration of a codeword, hence  $\mathbf{H}_n = \mathbf{H}$  for  $n = 1, \dots, N$ . Denote the difference of two codeword matrices with  $\Delta = [\Delta_1, \dots, \Delta_N]$ . Then, the argument of the MGF in Equation (4.4) can be described in terms of  $\mathbf{R}_{\text{Rx}}$  and  $\mathbf{R}_{\text{Tx}}$ .

$$\begin{aligned} \sum_{n=1}^N \|\mathbf{H}_n \Delta_n\|^2 &= \|\mathbf{H} \Delta\|^2 = \text{tr}(\mathbf{H} \Delta \Delta^H \mathbf{H}^H) \\ &= \text{vec}(\mathbf{H}^H)^H (\mathbf{I}_{n_R} \otimes \Delta \Delta^H) \text{vec}(\mathbf{H}^H) \\ &= \text{vec}(\tilde{\mathbf{H}}^H)^H \mathbf{R}_s^{1/2} (\mathbf{I}_{n_R} \otimes \Delta \Delta^H) \mathbf{R}_s^{H/2} \text{vec}(\tilde{\mathbf{H}}^H) . \end{aligned} \quad (4.5)$$

where  $\mathbf{R}_s$  is the covariance matrix of  $\text{vec}(\mathbf{H}^H)$  which leads to  $\mathbf{R}_s = \mathbf{R}_{\text{Rx}} \otimes \mathbf{R}_{\text{Tx}}$  (refer to Chapter 3). We wish to calculate the MGF of the above random variable, which consists of a positive semi-definite quadratic form involving Gaussian vectors  $\text{vec}(\tilde{\mathbf{H}}^H)$ . We now use the following result.

**Fact** [35]: Let  $\mathbf{A}$  be a Hermitian matrix and  $\mathbf{u}$  a circularly symmetric complex Gaussian vector with mean  $\bar{\mathbf{u}}$  and covariance matrix  $\mathbf{R}_{\mathbf{u}}$ . The MGF of the quadratic form  $y = \mathbf{u} \mathbf{A} \mathbf{u}^H$  is given as

$$\Phi_y(s) = \int_0^\infty e^{-sy} p_Y(y) dy = \frac{\exp(-\bar{\mathbf{u}} \mathbf{A} (\mathbf{I} - s \mathbf{R}_{\mathbf{u}} \mathbf{A})^{-1} \bar{\mathbf{u}}^H)}{|\mathbf{I} - s \mathbf{R}_{\mathbf{u}} \mathbf{A}|} , \quad (4.6)$$

where  $\mathbf{I}$  is the identity matrix with appropriate size.

□

Clearly  $\mathbf{u} = \text{vec}(\tilde{\mathbf{H}}^H)^H$  is a zero-mean Gaussian vector with covariance matrix  $\mathbf{R}_{\mathbf{u}} = \mathbf{I}_{n_T n_R}$  and  $\mathbf{R}_s^{1/2}(\mathbf{I}_{n_R} \otimes \Delta \Delta^H) \mathbf{R}_s^{H/2}$  is a Hermitian matrix, hence

$$\begin{aligned} \Phi(s) &= \left| \mathbf{I}_{n_R n_T} - s \mathbf{R}_s^{1/2} (\mathbf{I}_{n_R} \otimes \Delta \Delta^H) \mathbf{R}_s^{H/2} \right|^{-1} = \left| \mathbf{I}_{n_R n_T} - s (\mathbf{I}_{n_R} \otimes \Delta \Delta^H) \mathbf{R}_s \right|^{-1}, \\ &= \left| \mathbf{I}_{n_R n_T} - s (\mathbf{I}_{n_R} \otimes \Delta \Delta^H) (\mathbf{R}_{\text{Rx}} \otimes \mathbf{R}_{\text{Tx}}) \right|^{-1}, \end{aligned} \quad (4.7)$$

$$\begin{aligned} &= \left| \mathbf{I}_{n_R n_T} - s \mathbf{R}_{\text{Rx}} \otimes (\Delta \Delta^H \mathbf{R}_{\text{Tx}}) \right|^{-1}, \\ &= \prod_{i=1}^{n_T} \prod_{j=1}^{n_R} (1 - s \lambda_j^{(r)} \mu_i)^{-1}, \end{aligned} \quad (4.8)$$

where  $\lambda_j^{(r)}$  are the eigenvalues of  $\mathbf{R}_{\text{Rx}}$  and  $\mu_i$  are the eigenvalues of  $\Delta \Delta^H \mathbf{R}_{\text{Tx}}$ . Therefore the PEP in quasi-static case is

$$P(\mathbf{x} \rightarrow \hat{\mathbf{x}}) = \frac{1}{\pi} \int_0^{\frac{\pi}{2}} \left| \mathbf{I}_{n_R n_T} + \frac{E_s}{4N_0 \sin^2 \theta} \mathbf{R}_{\text{Rx}} \otimes (\Delta \Delta^H \mathbf{R}_{\text{Tx}}) \right|^{-1} d\theta \quad (4.9)$$

$$\leq \frac{1}{2} \left| \mathbf{I}_{n_R n_T} + \frac{E_s}{4N_0} \mathbf{R}_{\text{Rx}} \otimes (\Delta \Delta^H \mathbf{R}_{\text{Tx}}) \right|^{-1}, \quad (4.10)$$

where in Equation (4.10) we have the Chernoff bound for the PEP.

Other attempts have been made to understand and quantify the performance of spatially correlated MIMO channels in quasi-static fading; we briefly mention them and their relationship to our results. For the special case of i.i.d. channel substitute  $\mathbf{R}_{\text{Tx}} = \mathbf{I}_{n_T}$  and  $\mathbf{R}_{\text{Rx}} = \mathbf{I}_{n_R}$  in (4.9) to obtain an expression whose integral kernel is  $|\mathbf{I}_{n_T} - s \Delta \Delta^H|^{-n_R}$ . This special case has been reported in [28, 36]. Bölcskei and Paulraj [7] offer a different but equivalent expression for the same Chernoff bound. Liu and Sayeed [23] have reported the Chernoff bound corresponding to Equation (4.7).

It is insightful to approximate the Chernoff bound for the high-SNR region as in [34, 7]. Substituting (4.8) in (4.4) gives an alternative Chernoff bound which in high SNR takes the form

$$P(\mathbf{x} \rightarrow \hat{\mathbf{x}}) \leq \frac{1}{2} \left( \frac{E_s}{4N_0} \right)^{-r \hat{r}} \prod_{i=1}^r \prod_{j=1}^{\hat{r}} \frac{1}{\lambda_j^{(r)} \mu_i} \quad (4.11)$$

where  $r = \text{rank}(\mathbf{\Delta}\mathbf{\Delta}^H\mathbf{R}_{\text{Tx}})$  and  $\hat{r} = \text{rank}(\mathbf{R}_{\text{Rx}})$ . Whenever there is no transmit correlation, i.e.  $\mathbf{R}_{\text{Tx}} = \mathbf{I}_{n_T}$  and  $\mu_i = 1$ , expression (4.11) becomes equivalent to the one reported in [7].

In the high-SNR regime, the quality of a code is usually analyzed via the diversity order and the coding gain [34]. The diversity order of a pair of codewords is the exponent of SNR, i.e.  $r\hat{r} = \text{rank}(\mathbf{\Delta}\mathbf{\Delta}^H\mathbf{R}_{\text{Tx}}) \cdot \text{rank}(\mathbf{R}_{\text{Rx}})$  in Equation (4.11). Thus, the rank of receiver correlation appears directly, while the transmit correlation appears via  $r \leq \min\{\text{rank}(\mathbf{R}_{\text{Tx}}), \text{rank}(\mathbf{\Delta}\mathbf{\Delta}^H)\}$ .

### 4.3 Fast fading with spatial correlation

We consider the case where  $\mathbf{H}_n$  are independent for different  $n$ , but the entries of each matrix  $\mathbf{H}_n$  are correlated. In this case, the unconditional PEP can be calculated as follows

$$P(\mathbf{x} \rightarrow \hat{\mathbf{x}}) = \frac{1}{\pi} \int_0^{\frac{\pi}{2}} \prod_{n=1}^N \Phi_n \left( -\frac{E_s}{4N_0 \sin^2 \theta} \right) d\theta, \quad (4.12)$$

where  $\Phi_n(\cdot)$  is MGF of the random variable  $\|\mathbf{H}_n\mathbf{\Delta}_n\|^2$ . Similarly to the quasi-static case, we use the concept of a virtual (innovations) channel and a diagonalizing argument to arrive at a useful expression for the PEP.

$$\begin{aligned} \Phi_n(s) &= |\mathbf{I}_{n_R n_T} - s(\mathbf{I}_{n_R} \otimes \mathbf{\Delta}_n \mathbf{\Delta}_n^H) \mathbf{R}_s|^{-1} \\ &= |\mathbf{I}_{n_R n_T} - s \mathbf{R}_{\text{Rx}} \otimes (\mathbf{\Delta}_n \mathbf{\Delta}_n^H \mathbf{R}_{\text{Tx}})|^{-1} \\ &= \prod_{i=1}^{n_T} \prod_{j=1}^{n_R} \left( 1 - s \lambda_j^{(r)} \mu_{n,i} \right)^{-1} \end{aligned} \quad (4.13)$$

$$P(\mathbf{x} \rightarrow \hat{\mathbf{x}}) = \frac{1}{\pi} \int_0^{\frac{\pi}{2}} \prod_{n=1}^N \prod_{i=1}^{n_T} \prod_{j=1}^{n_R} \left( 1 + \frac{E_s}{4N_0 \sin^2 \theta} \lambda_j^{(r)} \mu_{n,i} \right)^{-1} d\theta \quad (4.14)$$

$$\leq \frac{1}{2} \prod_{n=1}^N \prod_{i=1}^{n_T} \prod_{j=1}^{n_R} \left( 1 + \frac{E_s}{4N_0} \lambda_j^{(r)} \mu_{n,i} \right)^{-1}, \quad (4.15)$$

where  $\mu_{n,i}$  are the eigenvalues of  $\mathbf{\Delta}_n \mathbf{\Delta}_n^H \mathbf{R}_{\text{Tx}}$ , and  $\lambda_j^{(r)}$  are the eigenvalues of  $\mathbf{R}_{\text{Rx}}$ . There are several differences between these expressions and those of the quasi-static case. First, unlike the quasi-static case, we observe time diversity (when  $\mathbf{\Delta}$  is nonzero). Second, only the rank of  $\mathbf{R}_{\text{Rx}}$  affects the overall diversity. The eigenvalues of  $\mathbf{R}_{\text{Rx}}$  affect the coding gain. Finally, the transmit correlation matrix affects the coding gain but not the diversity order.

It is insightful to evaluate (4.14) for the special case where the antennas are uncorrelated. Since  $\mathbf{\Delta}_n \mathbf{\Delta}_n^H$  has rank one and its only non-zero eigenvalue is  $\sum_{i=1}^{n_T} |x_i^{(n)} - \hat{x}_i^{(n)}|^2$  we have

$$\Phi_n(s) = |\mathbf{I}_{n_T} - s \mathbf{\Delta}_n \mathbf{\Delta}_n^H|^{-n_R} = \left( 1 - s \sum_{i=1}^{n_T} |x_i^{(n)} - \hat{x}_i^{(n)}|^2 \right)^{-n_R},$$

Substituting in (4.12) and setting  $s = -E_s/4N_0 \sin^2 \theta$  yields a result similar to the one reported in [28].

#### 4.4 Block fading with spatial correlation

The block fading model is a useful approximation for a time-varying fading channel when fading is not fast enough to be represented with a temporally i.i.d. process, but also not slow enough to be well approximated with a quasi-static model. The block fading model has been widely used in literature. In this model, the channel realization remains fixed for a time interval of length  $M$ . Subsequent time intervals are assumed to have independent realizations. Denoting the length of a codeword with  $N$ , we assume for simplicity that  $N = KM$ , i.e., that a codeword length consists of an integer number of block fading intervals.

To derive the PEP for block fading, we can use the procedures employed in the two cases of fast and quasi-static fading. Block fading consists of blocks of  $M$

samples that experience identical fading (like the quasi-static case), but on the other hand block fading also exhibits independence between fading blocks (like fast fading). Using a combination of the methods already described, we find the PEP under block fading as follows

$$\begin{aligned}
P(\mathbf{x} \rightarrow \hat{\mathbf{x}}) &= \frac{1}{\pi} \int_0^{\frac{\pi}{2}} \prod_{k=1}^K \left| \mathbf{I}_{n_R n_T} + \frac{E_s}{4N_0 \sin^2 \theta} \mathbf{R}_{\mathbf{R}_X} \otimes (\mathbf{\Delta}_k \mathbf{\Delta}_k^H \mathbf{R}_{\mathbf{T}_X}) \right|^{-1} d\theta \\
&= \frac{1}{\pi} \int_0^{\frac{\pi}{2}} \prod_{k=1}^K \prod_{i=1}^{n_T} \prod_{j=1}^{n_R} \left( 1 + \frac{E_s}{4N_0 \sin^2 \theta} \lambda_j^{(r)} \mu_{k,i} \right)^{-1} d\theta, \quad (4.16)
\end{aligned}$$

where  $\mathbf{\Delta}_k = [\mathbf{\Delta}_{k,1}, \dots, \mathbf{\Delta}_{k,M}]$ , and  $\mu_{k,i}$  are the eigenvalues of  $\mathbf{\Delta}_k \mathbf{\Delta}_k^H \mathbf{R}_{\mathbf{T}_X}$ . We notice that the time diversity in this case is at most  $K$ . Both  $\mathbf{R}_{\mathbf{R}_X}$  and  $\mathbf{R}_{\mathbf{T}_X}$  affect the overall diversity and coding gain.

#### 4.5 Temporal and spatial correlation

Block fading is only an approximation to the channel fading variations. In practice, channel variations are better described by sample-to-sample correlations. In many cases, due to size of codewords or other constraints, one may not be able to use interleaving, and temporal correlations must be accounted for. In this section we consider this general case.

For calculating pairwise error probabilities, we are interested in codeword coordinates where  $\mathbf{x}$  and  $\hat{\mathbf{x}}$  are not identical. Assume that among the  $N$  time indices, the two codewords  $\mathbf{x}$  and  $\hat{\mathbf{x}}$  are different in the time instances  $\{k_1, \dots, k_d\}$ . Let the channel matrix at time  $k_i$  be denoted as  $\mathbf{H}_i$ , and define  $\mathcal{H} = [\mathbf{H}_1, \dots, \mathbf{H}_d]$ . Each  $\mathbf{H}_i$  may be spatially correlated with  $\text{vec}(\mathbf{H}_i)$  modeled by a matrix  $\mathbf{R}_s = \mathbf{R}_{\mathbf{T}_X} \otimes \mathbf{R}_{\mathbf{R}_X}$ . We assume the statistics to be stationary (time-invariant), therefore only one spatial correlation matrix suffices. Let  $\mathbf{\Delta}_i = \mathbf{x}_{k_i} - \hat{\mathbf{x}}_{k_i}$  and  $\mathbf{\Lambda} = \text{diag}(\mathbf{\Delta}_1, \dots, \mathbf{\Delta}_d)$ . The PEP

for a given channel realization is

$$P(\mathbf{x} \rightarrow \hat{\mathbf{x}}|\mathbf{H}) = \frac{1}{\pi} \int_0^{\frac{\pi}{2}} \exp\left(-\frac{E_s}{4N_0 \sin^2 \theta} \|\mathcal{H}\boldsymbol{\Lambda}\|^2\right) d\theta ,$$

and the unconditional PEP:

$$P(\mathbf{x} \rightarrow \hat{\mathbf{x}}) = \frac{1}{\pi} \int_0^{\frac{\pi}{2}} \Phi\left(-\frac{E_s}{4N_0 \sin^2 \theta}\right) d\theta , \quad (4.17)$$

where  $\Phi(\cdot)$  is the MGF of the random variable  $\|\mathcal{H}\boldsymbol{\Lambda}\|^2$ . Assume that the temporal correlation of the channel are modeled by  $\mathbf{R}_t$ , that is,  $\mathbf{R}_t(i, j)$  is the correlation of the channel between two time instances  $i$  and  $j$ . After some algebra,  $\mathcal{H}$  can be described as follows

$$\mathcal{H} = \mathbf{R}_{\text{Rx}}^{1/2} \tilde{\mathcal{H}} (\mathbf{R}_t \otimes \mathbf{R}_{\text{Tx}})^{1/2} , \quad (4.18)$$

where  $\tilde{\mathcal{H}}$  is a  $(n_T n_R) \times d$  matrix with i.i.d. elements. Note that  $\text{vec}(\mathcal{H}^H) = \mathbf{R}^{1/2} \text{vec}(\tilde{\mathcal{H}}^H)$ , where  $\mathbf{R} = \mathbf{R}_{\text{Rx}} \otimes \mathbf{R}_t \otimes \mathbf{R}_{\text{Tx}}$ . Using arguments similar to those in Section 4.2, we obtain  $\Phi(\cdot)$  as follows

$$\begin{aligned} \Phi(s) &= \left| \mathbf{I}_{dn_T n_R} - s(\mathbf{I}_{n_R} \otimes \boldsymbol{\Lambda}\boldsymbol{\Lambda}^H)(\mathbf{R}_{\text{Rx}} \otimes \mathbf{R}_t \otimes \mathbf{R}_{\text{Tx}}) \right|^{-1} \\ &= \left| \mathbf{I}_{dn_T n_R} - s\mathbf{R}_{\text{Rx}} \otimes (\boldsymbol{\Lambda}\boldsymbol{\Lambda}^H(\mathbf{R}_t \otimes \mathbf{R}_{\text{Tx}})) \right|^{-1} \end{aligned} \quad (4.19)$$

We can substitute this expression in Equation (4.17) to obtain the appropriate PEP. High-SNR approximations of the Chernoff bound corresponding to this PEP can be used to develop design criteria for space-time codes in arbitrarily correlated channels, much the same way as done in [34].

To check the validity of this expression, we may specialize it to the uncorrelated case, i.e.  $\mathbf{R}_t = \mathbf{I}_d$ , leading to the result:

$$\Phi(s) = \prod_{n=1}^d \prod_{i=1}^{n_T} \prod_{j=1}^{n_R} \left(1 - s\lambda_j^{(r)} \mu_{n,i}\right)^{-1}$$

with  $\mu_{n,i}$  and  $\lambda_j^{(r)}$  defined as in Section 4.3. In deriving this expression we have used the following fact: the set of the eigenvalues of a Kronecker product of two matrices consists of products of all pairs of eigenvalues of the two matrices. Notice that the last expression has terms that are identical to Equation (4.13). Similarly, the results of this section specialize to the quasi-static case when we substitute the appropriate correlation matrix.

#### 4.6 Performance under Rician fading

The presence of a line-of-sight component creates a non-zero mean component for the complex Gaussian channel, leading to Rician fading. We denote the mean value of the matrix channel as  $\bar{\mathbf{H}}$ . The matrix channel can be represented as  $\bar{\mathbf{H}} + \mathbf{H}$ , where  $\mathbf{H}$  is a circularly symmetric complex Gaussian matrix. The innovations of the channel gain coefficients is calculated in the same manner as before to give  $\mathbf{R}_{\tilde{\mathbf{H}}} = \frac{1}{1+K} \mathbf{I}_{n_T n_R}$ , where  $K$  is the Rician factor.

Recall that the key to the developments for the Rayleigh case was an expression for the MGF of a quadratic form, namely Equation (4.6), which we repeat here for convenience

$$\Phi_y(s) = \int_0^\infty e^{-sy} p_Y(y) dy = \frac{\exp(-\bar{\mathbf{u}}\mathbf{A}(\mathbf{I} - s\mathbf{R}_{\mathbf{u}}\mathbf{A})^{-1}\bar{\mathbf{u}}^H)}{|\mathbf{I} - s\mathbf{R}_{\mathbf{u}}\mathbf{A}|}$$

In the previous cases, the complex channel coefficients were Gaussian with zero mean, therefore the numerator in the MGF expression was unity. In the present case, we can use the same expression and use the same procedures that were applied in Section 4.5, except that now the numerator does not simplify, and more calculations are necessary. In the following we omit the detailed calculations and give only the final PEP expressions.

For the quasi-static case, define  $\mathbf{\Gamma} = \mathbf{R}_s^{1/2}(\mathbf{I}_{n_R} \otimes \mathbf{\Delta}\mathbf{\Delta}^H)\mathbf{R}_s^{H/2}$ . Then

$$P(\mathbf{x} \rightarrow \hat{\mathbf{x}}) = \frac{1}{\pi} \int_0^{\frac{\pi}{2}} \frac{\exp\left(\text{vec}(\bar{\mathbf{H}}^H)^H \mathbf{\Gamma} (\mathbf{I}_{n_R n_T} + (E_s/4(1+K)N_0 \sin^2 \theta) \mathbf{\Gamma})^{-1} \text{vec}(\bar{\mathbf{H}}^H)\right)}{|\mathbf{I}_{n_R n_T} + (E_s/4(1+K)N_0 \sin^2 \theta) \mathbf{\Gamma}|} d\theta . \quad (4.20)$$

For the fast-fading case, let  $\mathbf{\Gamma}_n = \mathbf{R}_s^{1/2}(\mathbf{I}_{n_R} \otimes \mathbf{\Delta}_n \mathbf{\Delta}_n^H)\mathbf{R}_s^{H/2}$ . Then

$$P(\mathbf{x} \rightarrow \hat{\mathbf{x}}) = \frac{1}{\pi} \int_0^{\frac{\pi}{2}} \prod_{n=1}^N \frac{\exp\left(\text{vec}(\bar{\mathbf{H}}^H)^H \mathbf{\Gamma}_n (\mathbf{I}_{n_R n_T} + (E_s/4(1+K)N_0 \sin^2 \theta) \mathbf{\Gamma}_n)^{-1} \text{vec}(\bar{\mathbf{H}}^H)\right)}{|\mathbf{I}_{n_R n_T} + (E_s/4(1+K)N_0 \sin^2 \theta) \mathbf{\Gamma}_n|} d\theta . \quad (4.21)$$

One may verify the validity of (4.21) in the special case of uncorrelated channel, by setting  $\mathbf{\Gamma}_n = \mathbf{I}_{n_R} \otimes \mathbf{\Delta}_n \mathbf{\Delta}_n^H$ , which leads to a result that has been reported in [28].

For the spatially and temporally correlated Rician channel, using existing definitions, we present the following expression as the PEP

$$P(\mathbf{x} \rightarrow \hat{\mathbf{x}}) = \frac{1}{\pi} \int_0^{\frac{\pi}{2}} \frac{\exp\left(\text{vec}(\bar{\mathcal{H}}^H)^H \mathbf{\Gamma} (\mathbf{I}_{d_{n_R n_T}} + (E_s/4(1+K)N_0 \sin^2 \theta) \mathbf{\Gamma})^{-1} \text{vec}(\bar{\mathcal{H}}^H)\right)}{|\mathbf{I}_{d_{n_R n_T}} + (E_s/4(1+K)N_0 \sin^2 \theta) \mathbf{\Gamma}|} d\theta , \quad (4.22)$$

where  $\mathbf{\Gamma} = \mathbf{R}^{1/2}(\mathbf{I}_{n_R} \otimes \mathbf{\Lambda}\mathbf{\Lambda}^H)\mathbf{R}^{H/2}$ ,  $\mathbf{R} = \mathbf{R}_{\text{Rx}} \otimes \mathbf{R}_t \otimes \mathbf{R}_{\text{Tx}}$ .

## 4.7 Summary

In this chapter, we analyzed space-time codes under several channels. We considered Rayleigh as well as Rician channels. We also considered correlation between antennas, or correlation in time. Note that this analysis is applicable to all space-time codes. In Chapter 6 we apply this PEP expressions to space-time trellis codes, super-orthogonal codes and linear-dispersion codes.

## CHAPTER 5

### ANALYSIS OF CODED SPACE-TIME BLOCK TRANSMISSION

In this chapter, we provide analysis for a special case, that of concatenated channel codes and orthogonal space-time block codes. We use the equivalent SISO channel model and recognize that it is a block fading channel, to derive PEPs for spatially and temporally correlated and i.i.d. cases. We use the spatial correlation model developed in Chapter 3, and use unitary transformation on this channel to derive moment generating function.

#### 5.1 System model

We consider a coding-diversity scheme where a channel code and a STBC are used as shown in Figure 5.1. The channel code can be a single or concatenated code. The channel encoder maps a sequence of  $k$  information bits to  $n$  coded bits. Each coded bit is modulated by a signal with unit energy. This is further encoded by the space time block encoder with  $n_T$  transmit antennas. The receiver employs  $n_R$  receive antennas and combines their output optimally. We consider a frequency non-selective fading channel. The output of the channel is given by

$$\mathbf{y} = \mathbf{H} \mathbf{s} + \mathbf{n} \quad (5.1)$$

where  $\mathbf{y}$  is  $n_R \times 1$  received signal vector,  $\mathbf{s}$  is the modulated  $n_T \times 1$  vector transmitted over  $n_T$  transmit antennas. and  $\mathbf{n}$  is  $n_R \times 1$  i.i.d. Gaussian noise at the input of the antennas. The channel matrix is represented by  $\mathbf{H}$  whose elements  $h_{ij}$  are the

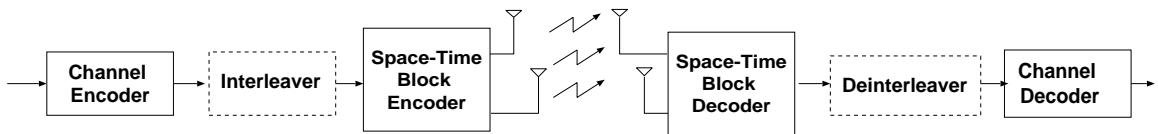


Figure 5.1. Concatenated channel code and space-time block code

complex Gaussian channel coefficients for the pair of transmit antenna  $i$  and receive antenna  $j$ .

In a STBC with  $n_T$  transmit antennas, it is assumed that the channel coefficients  $h_{ij}$  remain fixed through  $n_T$  consecutive intervals, and the receiver has either perfect or partial knowledge about them [1, 32]. Hence, the channel is block fading with block length  $n_T$ . Also, in the decoded sequence,  $n_T$  consecutive symbols are affected by the same set of fading coefficients  $h_{ij}$ 's.

The multiple-input multiple output channel, driven by an orthogonal STBC, can be represented by an equivalent single-input single-output (SISO) channel. Assuming the receiver combines the received signals from  $n_R$  antennas optimally, the MIMO channel can be represented as a SISO block fading channel with fading coefficient for each block of  $n_T$  symbols equal to:

$$h_{eq} = \sqrt{\frac{1}{n_T} \sum_{i=1}^{n_T} \sum_{j=1}^{n_R} |h_{ij}|^2}. \quad (5.2)$$

Alternately, we can write the equivalent SNR

$$\gamma = \bar{\gamma} \|H\|_F^2, \quad (5.3)$$

where  $\|\cdot\|_F$  denotes the Frobenius norm,  $\bar{\gamma} = \frac{1}{n_T} \frac{R_c E_b}{N_0}$  is the average SNR per information bit per transmit antenna, and  $R_c$  is the code rate.

If the noise components of the actual channel are independent, so are the noise components of the equivalent channel [3, 8]. The transmitted power is scaled

by the number of transmit antennas to keep the total transmitted power constant. The equivalent fading coefficient follows a generalized Rayleigh distribution [25]. The resultant instantaneous SNR per bit,  $\gamma$ , follows chi-square distribution with degree of freedom  $2n_T n_R$  [4].

The problem is now reduced to the analysis of a block fading SISO channel *which is no longer Rayleigh*, but rather follows a generalized Rayleigh distribution. Spatially correlated and temporally correlated channels, which we also consider in this work, further modify the probability distribution.

Here it is appropriate to make a note on interleaving. Some coded space-time transmission systems, e.g. [14], have been proposed that do not include interleaving between the outer and inner codes. However, our simulations show that the codes of [14] can be improved by 1.7dB with an interleaver<sup>1</sup>. Bauch and Hagenauer [3] also do not employ interleaving between inner and outer codes, where potentially similar gains in performance would be possible. In view of these gains and the relatively low cost of interleaving, it is important to include interleaving in the analysis of coded space-time systems.

Interleaving, however, requires a complicated and cumbersome book-keeping for calculating pairwise error probabilities. To manage this complexity and to avoid interleaver-dependent probabilities, we use the concept of a uniform interleaver. To demonstrate the efficacy of this approach, Figure 5.2 shows the pairwise error probability of the dominant error event (Hamming distance  $d = 5$ ) of a convolutional code concatenated with Alamouti signaling. The (averaged) uniform interleaver gives a good approximation to the best interleaver in realistic signal-to-noise ratios.<sup>2</sup> The us-

---

<sup>1</sup>See Chapter 6, Figure 6.7

<sup>2</sup>At very large SNR bad interleavers will dominate, hence averaging over all interleavers will eventually diverge from the best interleaver at arbitrarily large SNR. Nevertheless, it is an excellent

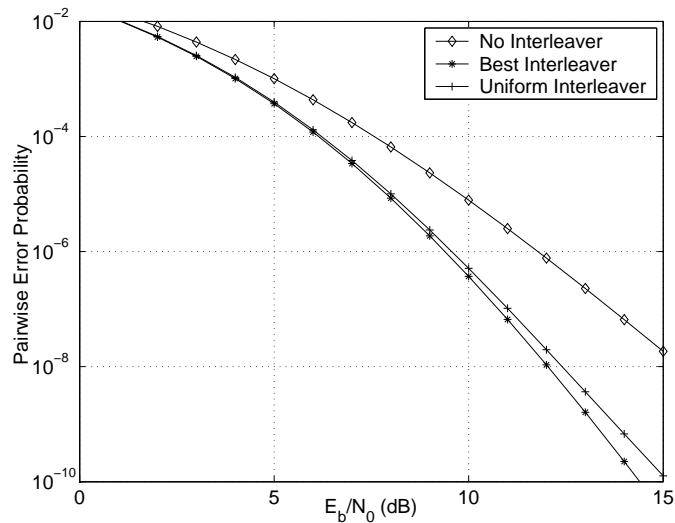


Figure 5.2. Convolutional Code, 2-Tx and 1-Rx antennas,  $d = 6$ , Block by block i.i.d. Rayleigh fading

age of random uniform interleaving was first proposed by Benedetto and Montorsi [6] for the analysis of turbo codes and has also been used by Zummo and Stark [38] to explore the effects of channel interleavers.

## 5.2 Analysis of block fading channel

The performance of channel codes in block fading environments is studied in [20, 24, 38]. The original analysis in [24] requires a generalized weight enumerating function of the channel code (or generalized transfer function for convolutional codes), which depends on the order of transmitted bits of a codeword. Therefore, the existence of interleaver complicates the analysis. We use the concept of *uniform interleaver* to address this problem in a manner closely following Zummo and Stark [38].

If the fading coefficient remains constant over a period of  $\ell$  symbols, the channel is called a block fading channel with block length  $\ell$ . Such a channel may arise in

---

approximation at moderate SNR.

practice if the coherence time of channel is greater than  $\ell$  symbols. However, block fading channels are only an approximation of time correlated channels. The channel coefficient is assumed to change independently from one block to another.

Assume that a frame of signals  $\{s_l\}_{l=1}^N$  is transmitted over block fading channel with block length  $\ell$ . The number of blocks  $F = \lceil \frac{N}{\ell} \rceil$ . The received signal is given by,

$$y_{f,l} = h_f s_{f,l} + n_{f,l} \quad f = 1, \dots, F \quad l = 1, \dots, \ell$$

where  $y_{f,l}$  and  $s_{f,l}$  are the  $l$ -th received and transmitted values in block  $f$  respectively.  $h_f$  is the channel coefficient in the corresponding block.

A maximum likelihood decoder will maximize the metric,

$$m(y, s) = \sum_f \sum_l |y_{f,l} - h_f s_{f,l}|^2 \quad (5.4)$$

From Equation 5.4 it is clear that the analysis required knowledge of distribution of coded symbols in the block  $f$ . This distribution is interleaver dependent, which makes the analysis harder. There have been several efforts to solve this problem.

The length of the coded sequence (frame length) is  $n$ . The length of a fading block is  $\ell$ , thus the number of fading blocks in each coded frame is  $F = \lceil n/\ell \rceil$ . We now need to determine how the error bits are distributed among different blocks, i.e., how much error weight is present in each fading block. To characterize that, we build a histogram of weights as follows: assume the number of blocks that have weight  $m$  is  $f_m$ , and consider the vector  $\mathbf{f} = (f_0, \dots, f_w)$  where  $w = \min(\ell, d)$ . A given vector  $\mathbf{f}$  is a valid histogram if  $\sum f_m = F$  and  $\sum m f_m = d$ .

For example, let the frame length be  $n = 5$  and fading block length be  $\ell = 2$ . If an error event with weight  $d = 4$  is interleaved, the following histograms are possible:  $(3, 0, 2), (2, 2, 1), (1, 4, 0)$ . It can be easily seen that the total number of

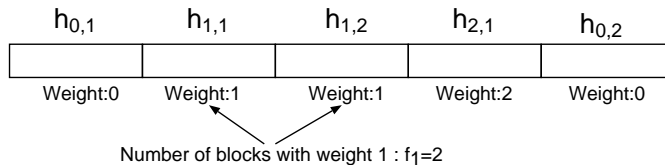


Figure 5.3. One possible block pattern for the case  $N = 5, d = 4, \ell = 2$

blocks is  $F = 5$ , and the total weight in each case is  $d = 4$ . The pattern  $(2, 2, 1)$  is shown in the Figure 5.3. Note that all the fading coefficients shown in the figure are independent.

Now, using the uniform interleaving concept, one may average the PEP over all valid error patterns (histograms).

$$P(d) = \mathcal{E}_{\mathbf{f}} [P(d|\mathbf{f})] = \sum_{f_1=1}^F \sum_{f_2=1}^{F/2} \dots \sum_{f_w=1}^{F/w} P(d|\mathbf{f})p(\mathbf{f}) \quad (5.5)$$

where  $\mathcal{E}$  is the expectation operator and,  $p(\mathbf{f})$  is the weight of occurrence of the pattern  $\mathbf{f}$  which can be found by combinatorics.

### 5.3 PEP based on moment generating functions

For a given channel code  $\mathcal{C}$ , assuming all-zero codeword is transmitted, the PEP of a codeword with weight  $d$  given the pattern  $\mathbf{f}$  of the fading blocks, is

$$P(d|\mathbf{f}, \gamma) = Q \left( \sqrt{2 \sum_{m=1}^w m \sum_{i=1}^{f_m} \gamma_{m,i}} \right) \quad (5.6)$$

Here we have collected terms corresponding to blocks with equal weight patterns. Thus  $\gamma_{m,i}$  is the SNR for the  $i$ -th block that has weight  $m$  (there are a total of  $f_m$  such blocks).<sup>3</sup>

<sup>3</sup>We use  $h_{ij}$  to refer to the channel gain from transmitter  $i$  to receiver  $j$ , whereas here the subscripts of  $\gamma_{m,i}$  have a very different meaning. Each case should be clear from the context.

In the case of  $n_T$  transmit and  $n_R$  receive antennas the resultant SNR per bit, from (5.2), is

$$\gamma = \bar{\gamma} \|\mathbf{H}\|_F^2 \quad (5.7)$$

where  $\bar{\gamma} = \frac{1}{n_T} \frac{R_c E_b}{N_0}$  is the average SNR per information bit, and  $R_c$  is the code rate. Representing Q-function in its alternative form [29], the PEP conditioned on the block fading pattern  $\mathbf{f}$  is

$$P(d|\mathbf{f}, \gamma) = \frac{1}{\pi} \int_0^{\frac{\pi}{2}} \exp\left(-\frac{1}{\sin^2 \theta} \sum_{m=1}^w m \sum_{i=1}^{f_m} \gamma_{m,i}\right) d\theta.$$

Averaging the above conditional PEP over the instantaneous SNR  $\gamma$  we find  $P(d|\mathbf{f}) = \mathcal{E}_\gamma [P(d|\mathbf{f}, \gamma)]$ . Assuming  $\gamma_{m,i}$  are independent,

$$P(d|\mathbf{f}) = \frac{1}{\pi} \int_0^{\frac{\pi}{2}} \prod_{m=1}^w \prod_{i=1}^{f_m} \int_0^\infty \exp\left(-\frac{m\gamma_{m,i}}{\sin^2 \theta}\right) p_\gamma(\gamma_{m,i}) d\gamma_{m,i} d\theta$$

The inner integral is the moment generating function (MGF) of  $\gamma$ ,  $\Phi(s) = \mathcal{E}[e^{s\gamma}]$ , evaluated at  $s = -m/\sin^2 \theta$ , hence

$$P(d|\mathbf{f}) = \frac{1}{\pi} \int_0^{\frac{\pi}{2}} \prod_{m=1}^w \left[ \Phi\left(-\frac{m}{\sin^2 \theta}\right) \right]^{f_m} d\theta. \quad (5.8)$$

The expression (5.8) is general for all the channels. In the sequel, we use moment generating function of different channels with expression (5.8) to derive pairwise error probabilities.

We start our analysis with spatially and temporally independent fading.

#### 5.4 Independent fading

If the entries of the channel matrix  $\mathbf{H}$  are independent, the resulting SNR is the sum of  $n_T n_R$  independent exponential variables and hence has a chi-square

distribution with the pdf [29]

$$p_\gamma(\gamma) = \frac{1}{(D-1)!\bar{\gamma}^D} \gamma^{D-1} \exp(-\gamma/\bar{\gamma}) ,$$

where  $D = n_T n_R$ . The MGF of this pdf is given by [29]

$$\Phi_\gamma(s) = (1 - s\bar{\gamma})^{-D} . \quad (5.9)$$

Using this MGF in (5.8) we obtain the following bound for  $P(d|\mathbf{f})$

$$\begin{aligned} P(d|\mathbf{f}) &= \frac{1}{\pi} \int_0^{\frac{\pi}{2}} \prod_{m=1}^w \left(1 + \frac{m\bar{\gamma}}{\sin^2 \theta}\right)^{-f_m D} d\theta \\ &\leq \frac{1}{2} \prod_{m=1}^w (1 + m\bar{\gamma})^{-f_m D} , \end{aligned} \quad (5.10)$$

where the last inequality is the Chernoff bound. One may also obtain the corresponding result for quasi-static Rayleigh fading by the setting  $F = 1$  which is equivalent to  $m = d$ ,  $f_m = 1$ .

## 5.5 Spatially correlated fading

**Theorem 1** *The moment generating function of  $\gamma$  is given by*

$$\Phi_\gamma(s) = \prod_{i=1}^{n_T} \prod_{j=1}^{n_R} \left(1 - s\lambda_i^{(t)}\lambda_j^{(r)}\bar{\gamma}\right)^{-1} , \quad (5.11)$$

where  $\lambda^{(t)}$  and  $\lambda^{(r)}$  are eigenvalues of  $\mathbf{R}_{Tx}$  and  $\mathbf{R}_{Rx}$  respectively.

**Proof:**

$$\begin{aligned} \|\mathbf{H}\|^2 &= \text{vec}(\mathbf{H})^H \text{vec}(\mathbf{H}) = \text{vec}(\tilde{\mathbf{H}})^H \Lambda \text{vec}(\tilde{\mathbf{H}}) \\ &= \sum_{i=1}^{n_T} \sum_{j=1}^{n_R} \lambda_i^{(t)} \lambda_j^{(r)} |\tilde{h}_{ij}|^2 . \end{aligned} \quad (5.12)$$

From (5.7) and (5.12),

$$\gamma = \bar{\gamma} \|\mathbf{H}\|^2 = \bar{\gamma} \sum_{i=1}^{n_T} \sum_{j=1}^{n_R} \lambda_i^{(t)} \lambda_j^{(r)} |\tilde{h}_{ij}|^2 .$$

The MGF of  $\gamma$  is

$$\Phi_\gamma(s) = \mathcal{E} \left\{ \exp \left( -s \bar{\gamma} \|\mathbf{H}\|^2 \right) \right\} = \prod_{i=1}^{n_T} \prod_{j=1}^{n_R} \mathcal{E} \left\{ \exp \left( -s \bar{\gamma} \lambda_i^{(t)} \lambda_j^{(r)} |\tilde{h}_{ij}|^2 \right) \right\} .$$

Each term in the last expression is the moment generating function of an exponential random variable. Substitution gives (5.11). □

We can now substitute in (5.8) to obtain

$$P(d|\mathbf{f}) = \frac{1}{\pi} \int_0^{\frac{\pi}{2}} \prod_{m=1}^w \prod_{i=1}^{n_T} \prod_{j=1}^{n_R} \left( 1 + \frac{m \lambda_i^{(r)} \lambda_j^{(r)} \bar{\gamma}}{\sin^2 \theta} \right)^{-f_m} d\theta \quad (5.13)$$

$$\leq \frac{1}{2} \prod_{m=1}^w \prod_{i=1}^{n_T} \prod_{j=1}^{n_R} \left( 1 + m \lambda_i^{(t)} \lambda_j^{(r)} \bar{\gamma} \right)^{-f_m} . \quad (5.14)$$

Using this formula, it is instructive to consider two extreme cases: uncorrelated and fully correlated channels. In the case of uncorrelated channel,  $\lambda_i^{(t)} = \lambda_j^{(r)} = 1$  for all  $i, j$ , and the formula reduces to (5.10), as expected. In the case of fully correlated channel, the correlation matrix is rank deficient and we have  $\lambda_1^{(t)} = n_T$ ,  $\lambda_1^{(r)} = n_R$ , and all other  $\lambda_i^{(t)} = \lambda_j^{(r)} = 0$ . Thus the above moment generating function reduces to

$$\Phi_\gamma(s) = (1 - sD\bar{\gamma})^{-1} , \quad (5.15)$$

which shows no diversity, but a receive gain of  $D = n_T n_R$  (recall that  $\bar{\gamma} = \frac{1}{n_T} \frac{R_c E_b}{N_0}$ ).

## 5.6 Temporal and spatial correlation

For various reasons such as long data blocks or long fading periods, it may not be practical to use interleavers to remove the channel memory. In such cases, we

need to analyze the system with channel memory, a task which we undertake in this section. We assume that the coherence time is much greater than  $n_T$  symbols, so that the channel remains effectively constant over each STBC block and linear decoding is possible.

Assuming a given error event has weight  $d$ , we must concentrate on the channel matrix at time instances  $\{k_1, \dots, k_d\}$  where the error event has nonzero value. Let the channel matrix at time  $k_i$  be denoted as  $\mathbf{H}_i$  and define  $\mathcal{H} = [\text{vec}(\mathbf{H}_1) \text{vec}(\mathbf{H}_2) \dots \text{vec}(\mathbf{H}_d)]$ . Each  $\mathbf{H}_i$  may be spatially correlated; the spatial correlations are modeled by a matrix  $\mathbf{R}_s$  as before. We assume the statistics to be stationary (time-invariant), therefore only one spatial correlation matrix suffices. We model the temporal correlation of the channel by  $\mathbf{R}_t$ , that is,  $\mathbf{R}_t(i, j) = \mathcal{E}[\text{vec}(\mathbf{H}_i)^H \text{vec}(\mathbf{H}_j)]$ . Therefore,  $\mathcal{H}$  can be modeled as

$$\mathcal{H} = \mathbf{R}_s^{1/2} \tilde{\mathcal{H}} \mathbf{R}_t^{1/2} \quad , \quad (5.16)$$

where,  $\tilde{\mathcal{H}}$  is a  $(n_T n_R) \times d$  matrix with i.i.d. elements.

Using Lemmas 1 and 1, we can write the MGF of  $d n_T n_R$  correlated exponential variables as

$$\Phi_\gamma(s) = \prod_{k=1}^d \prod_{i=1}^{n_T} \prod_{j=1}^{n_R} (1 - s \mu_k \lambda_i^{(t)} \lambda_j^{(r)})^{-1} \quad , \quad (5.17)$$

where  $\mu_i$  are eigenvalues of  $\mathbf{R}_t$ . Using this, we can calculate the pairwise error probability

$$P(d) = \frac{1}{\pi} \int_0^{\pi/2} \prod_{k=1}^d \prod_{i=1}^{n_T} \prod_{j=1}^{n_R} \left( 1 + \frac{\bar{\gamma} \mu_k \lambda_i^{(t)} \lambda_j^{(r)}}{\sin^2 \theta} \right)^{-1} d\theta \quad (5.18)$$

$$\leq \frac{1}{2} \prod_{k=1}^d \prod_{i=1}^{n_T} \prod_{j=1}^{n_R} \left( 1 + \mu_k \lambda_i^{(t)} \lambda_j^{(r)} \bar{\gamma} \right)^{-1} \quad . \quad (5.19)$$

It is easy to see that for the special case of quasi-static fading,  $(\mathbf{R}_t)_{ij} = 1$  for all  $i$  and  $j$ , therefore  $\mu_1 = d$  and all other  $\mu_k = 0$ , and the equation reduces to the familiar PEP for the quasi-static fading, where there is no time diversity but there is a coding gain of  $d$ .

## 5.7 Performance analysis with multilevel modulation

We now proceed to the analysis of a concatenation of TCM or MTCM with space-time block codes. The design of TCM and MTCM for space-time block codes has been addressed in [14] and [8].

Following the same steps as before, we need to consider error patterns  $\mathbf{f}$  (histograms) in a manner similar to Section 5.2. Because the errors can assume multiple values (more than two), the construction of the patterns is complicated. In a  $2^m$ -ary modulation, an error event can be represented by  $\mathbf{d} = (d_0, \dots, d_{2^m-1})$ , where  $d_i$  is the number of times  $i$ -th symbol repeats in the error event. Obviously,  $\sum_{i=0}^{2^m-1} d_i = N$  the codeword length. As in Section 5.2, we denote number of fading blocks with  $F$  and block length with  $\ell$ . Then fading pattern in block  $j$  can be given by  $\mathbf{v}_j = (v_j^{(0)}, \dots, v_j^{(2^m-1)})$ , where  $v_j^{(i)}$  is the number of times symbol  $i$  repeats in that particular block. A histogram  $\mathbf{f} = \{f_j : \mathbf{v}_j \text{ repeats } f_j \text{ times}\}$  is a valid histogram if:

$$\sum_j f_j = F \quad , \quad \sum_j f_j v_j^{(i)} = d_i \quad , \quad i = 0, \dots, 2^m - 1$$

For example, let the error event (compared to all zero codeword) in a TCM with QPSK modulation and codeword length  $N = 8$  be  $\{s_2, s_1, s_0, s_3, s_1, s_2, s_0, s_1\}$ . Obviously  $\mathbf{d} = (2, 3, 2, 1)$ . If the block length is 2, the distribution of errors can be given as follows,

	$j = 1$	$j = 2$	$j = 3$	$j = 4$
	$s_2s_1$	$s_0s_3$	$s_1s_2$	$s_0s_1$
$v_j^{(0)}$	0	1	0	1
$v_j^{(1)}$	1	0	1	1
$v_j^{(2)}$	1	0	1	0
$v_j^{(3)}$	0	1	0	0

Hence, In the first block,  $v_j = (0, 1, 1, 0)$ , in the second block  $v_j = (1, 0, 0, 1)$  etc. The above block distribution can be represented by the histogram:

$\mathbf{v}_j$	$f_j$
(0, 1, 1, 0)	2
(1, 0, 0, 1)	1
(1, 1, 0, 0)	1
(2, 3, 2, 1)	$= \sum_j f_j v_j^{(i)}$

The pairwise conditional probability of error between the all-zero codeword and a codeword  $\mathbf{e}$  is given by,

$$P(\mathbf{0} \rightarrow \mathbf{e} | \mathbf{f}, \gamma) = Q \left( \sqrt{2 \sum_j \sum_{i=1}^{f_j} \gamma_{j,i} \alpha_j} \right) , \quad (5.20)$$

where  $j$  is the index of block patterns and  $\gamma_{j,i}$  is the instantaneous SNR per bit for  $i$ -th block in fading pattern  $j$ . We have defined an aggregate distance metric  $\alpha_j$  for each block pattern  $j$ , calculated by

$$\alpha_j = \sum_{k=0}^{2^m} v_j^{(k)} d^2(s_k, s_0) ,$$

where  $v_j^{(k)}$  is the multiplicity of symbol  $s_k$  in the block pattern indexed by  $j$ . Averaging over  $\gamma$ , we find the PEP expression

$$P(\mathbf{0} \rightarrow \mathbf{e} | \mathbf{f}) = \frac{1}{\pi} \int_0^{\pi/2} \prod_j \left[ \Phi_\gamma \left( -\frac{\alpha_j}{2 \sin^2 \theta} \right) \right]^{f_j} d\theta . \quad (5.21)$$

For the useful class of uniform error probability (UEP) codes, where the reference codeword can always be chosen as the all-zero codeword [29, 19], the union bound on frame error probability is

$$P_e \leq \sum_{\mathbf{e} \neq \mathbf{0}} \frac{1}{\pi} \int_0^{\frac{\pi}{2}} \prod_j \left( 2^{-(m-1)} \sum_{c_\ell} \Phi_\gamma \left( -\frac{\sum_{i=1}^{2^m} v_j^{(i)} d^2(c_\ell \oplus s_i, s_i)}{2 \sin^2 \theta} \right)^{-f_j} \right) d\theta, \quad (5.22)$$

where  $c_\ell$  is a symbol that belongs to the first level of set-partitioning of the  $2^m$ -ary modulation [19]. Note that  $v_j^{(i)}$  and  $f_j$  depend on the error word  $\mathbf{e}$ , but the dependence has been suppressed in the formula above for notational simplicity.

To calculate the union bound in the case of spatially and temporally i.i.d. fading, the moment generating function (5.9) is substituted in (5.22). To calculate the union bound in the case of spatially correlated fading, we insert the moment generating function (5.11) into (5.21).

The union bound in the case of temporally correlated channel requires a little twist. In the previous cases, the equivalent SNR was a function of  $\|\mathbf{H}\|$  only, therefore decorrelating  $\mathbf{H}$  simplified the MGF expressions. However, in the case of temporal correlations, the effective SNR is expressed as

$$\gamma = \sum_{k=1}^d \sum_{i=1}^{n_T} \sum_{j=1}^{n_R} |h_{ij}(k)|^2 \delta_k^2, \quad (5.23)$$

where  $\delta_k$  is the Euclidean distance of the error event at  $k$ -th error position. Obviously decorrelating  $\mathbf{H}$  no longer works. Define  $\mathbf{D} = \text{diag}(\delta_1, \dots, \delta_d)$  and note that  $\gamma = \|\mathcal{H}\mathbf{D}\|^2$ , where  $\mathcal{H} = [\text{vec}(\mathbf{H}_1) \text{vec}(\mathbf{H}_2) \dots \text{vec}(\mathbf{H}_d)]$ . To obtain a sum of independent SNR components, we must diagonalize the autocorrelation of  $\mathcal{H}\mathbf{D}$ .

$$\begin{aligned} \gamma = \|\mathcal{H}\mathbf{D}\|^2 &= \sum_{k=1}^d \sum_{i=1}^{n_T} \sum_{j=1}^{n_R} |h_{ij}(k)|^2 \delta_k^2 \\ &= \sum_{k=1}^d \sum_{i=1}^{n_T} \sum_{j=1}^{n_R} |\tilde{h}_{ij}(k)|^2 \lambda_i^{(t)} \lambda_j^{(r)} \hat{\mu}_k. \end{aligned}$$

Recall that the spatial and temporally correlated  $\mathcal{H}$  is modeled as

$$\mathcal{H} = \mathbf{R}_s^{1/2} \tilde{\mathcal{H}} \mathbf{R}_t^{1/2} ,$$

where  $\tilde{\mathcal{H}}$  has i.i.d. entries and  $\mathbf{R}_s$  and  $\mathbf{R}_t$  are the spatial and temporal correlation matrices, respectively. It follows that  $\hat{\mu}_k$  are the eigenvalues of  $\mathbf{D}\mathbf{R}_t\mathbf{D}$ . Therefore we can still use equations (5.17) and (5.21) except we should substitute  $\hat{\mu}_k$  for  $\mu_k$ .<sup>4</sup>

## 5.8 Performance under Rician fading

In this section we consider the Rician fading channels with parameter  $K$  describing the ratio of the energy of the line-of-sight component to the multipath component. For the uncorrelated Rician channel, the moment generating function of  $\gamma = \bar{\gamma}||H||^2$  is given by [29]

$$\Phi_\gamma(s) = \left( \frac{1+K}{1+K-s\bar{\gamma}} \right)^D \exp \left( \frac{Ks\bar{\gamma}}{1+K-s\bar{\gamma}} \right)^D .$$

By using this MGF with equation (5.21), the PEP for the fast fading Rician channel and multilevel modulation is given by

$$P(\mathbf{0} \rightarrow \mathbf{e}) = \frac{1}{\pi} \int_0^{\pi/2} \prod_j \left[ \frac{1+K}{1+K+\frac{\alpha_j\bar{\gamma}}{2\sin^2\theta}} \exp \left( -\frac{K\frac{\bar{\gamma}\alpha_j}{2\sin^2\theta}}{1+K+\frac{\bar{\gamma}\alpha_j}{2\sin^2\theta}} \right) \right]^D d\theta . \quad (5.24)$$

For the case of spatially correlated fading, the MGF can be once again derived using Lemmas 1 of Section 3.1 and Lemma 2 of Section 5.5,

$$\Phi_\gamma(s) = \prod_{i=1}^{n_T} \prod_{j=1}^{n_R} \frac{(1+K)}{1+K-s\lambda_i^{(t)}\lambda_j^{(r)}\bar{\gamma}} \exp \left( \frac{Ks\lambda_i^{(t)}\lambda_j^{(r)}\bar{\gamma}}{1+K-s\lambda_i^{(t)}\lambda_j^{(r)}\bar{\gamma}} \right) , \quad (5.25)$$

---

<sup>4</sup>The distinction is unnecessary in the case of binary codes with BPSK, because in that case  $\delta_k = 1$  on all error positions.

where  $\lambda^{(t)}$  and  $\lambda^{(r)}$  are the eigenvalues of transmit and receive correlation matrices  $\mathbf{R}_{\text{Tx}}$  and  $\mathbf{R}_{\text{Rx}}$  respectively. Expressions (5.25) and (5.22) directly yield the desired bounds on error probability.

When temporal as well as spatial correlation is present, it is straightforward to show that the moment generating function is expressed as follows

$$\Phi_{\gamma}(s) = \prod_{k=1}^d \prod_{i=1}^{n_T} \prod_{j=1}^{n_R} \frac{(1+K)}{1+K-s\mu_k\lambda_i^{(t)}\lambda_j^{(r)}\bar{\gamma}} \exp\left(\frac{Ks\mu_k\lambda_i^{(t)}\lambda_j^{(r)}\bar{\gamma}}{1+K-s\mu_k\lambda_i^{(t)}\lambda_j^{(r)}\bar{\gamma}}\right), \quad (5.26)$$

where  $\mu_k$  are the eigenvalues of temporal correlation matrix  $\mathbf{R}_t$ . Once again, in combination with (5.22), the desired bounds are obtained.

## 5.9 Summary

In this chapter, we derived the PEP expression for concatenated channel codes and space-time block codes. This setup provides full diversity and coding gain with simple design, at the cost of losing some rate. We analyzed this system for spatially and/or temporally correlated channels as well as i.i.d. channels. We also provided analysis for Rayleigh and Rician fading. In the next chapter, we use PEP expression derived in Chapters 4 and 5 to calculate union bounds on bit and frame error probabilities.

## CHAPTER 6

### APPLICATIONS AND RESULTS

We apply the PEP expressions derived in the Chapters 5 and 4 to various space-time codes. This chapter is divided into two parts. The first part gives the results for concatenated channel codes and orthogonal space-time block codes. We provide results for various channel codes like convolutional codes, turbo codes, TCM and MTCM concatenated with OSTBC. In the second part we provide the results for space-time trellis codes, super-orthogonal space-time codes, and linear-dispersion codes.

#### 6.1 Coded space-time block signaling

We evaluated union bounds for convolutional and turbo codes with BPSK modulation, and for 4-state, 8-PSK TCM and MTCM codes. The STBC for two-transmit antenna used here is the Alamouti scheme [1]. In all figures, dashed lines denote simulations, while solid lines denote bounds. In the case of two antennas,  $\mathbf{R}_{\text{Tx}}$  and  $\mathbf{R}_{\text{Rx}}$  are each fully defined by a single correlation coefficient  $\rho_t$  for transmit antenna and  $\rho_r$  for receive antenna. To evaluate analytical expressions, we calculated the IOWEF of the codes based on the approach of [5]. A random interleaver is placed between the channel code and STBC. We evaluate exact expressions for pairwise error probability.

We begin by presenting our results for convolutional codes. For this experiment, we used a four-state rate-1/2 code with generator function  $G(D) = (1 + D^2, 1 +$

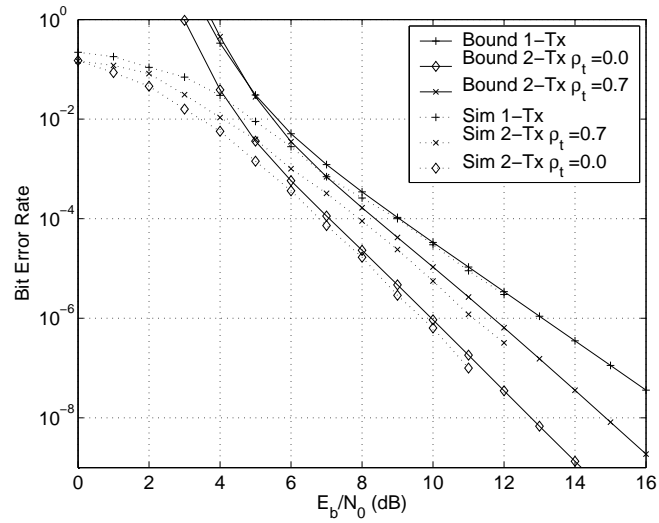


Figure 6.1. Convolutional code, block i.i.d. Rayleigh Fading, 2-Tx and 1-Rx antennas

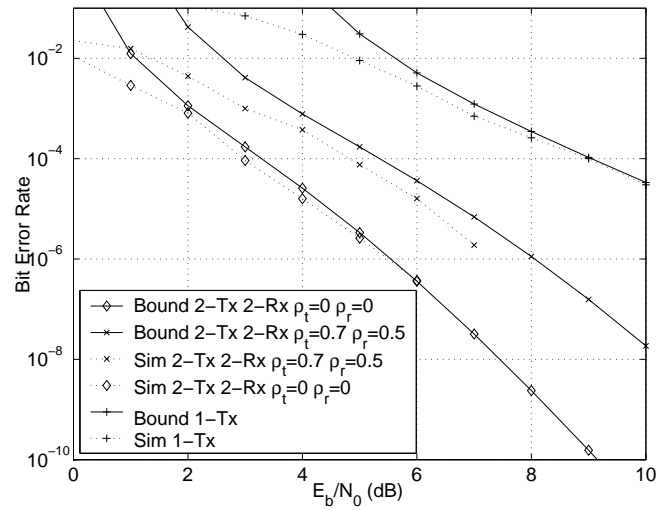


Figure 6.2. Convolutional code, block i.i.d. Rayleigh Fading, 2-Tx and 2-Rx antennas

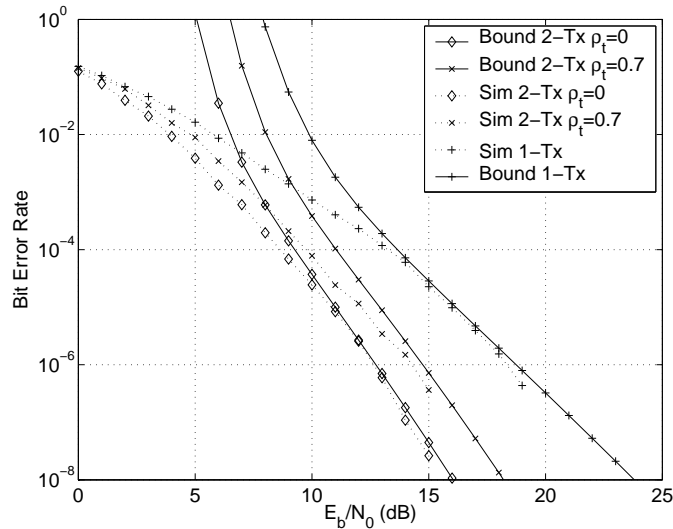


Figure 6.3. Convolutional code, 2-Tx and 1-Rx antennas, time correlated Rayleigh Fading,  $F_d T_s = 0.1$

$D^2 + D^3$ ). Each frame contains  $k = 100$  information bits (200 BPSK symbols). This code is concatenated with Alamouti STBC (one receive antenna). The results are shown in Figure 6.1. When there is no correlation between antennas, the diversity is two. When the correlation between transmit antennas is  $\rho_t = 0.7$ , the diversity remains the same, but the loss in coding gain is about 1.5dB at BER=  $10^{-5}$ . We next consider a system with two transmit and two receive antennas with spatial correlations  $\rho_t = 0.7$  and  $\rho_r = 0.5$  (Figure 6.2). We observe that receive diversity improves the overall performance, but the loss due to antenna correlations is more than 2dB at BER= $10^{-5}$ .

In our final experiment with convolutional codes (Figure 6.3) we demonstrate the effect of temporal correlation modeled via Bessel functions [31] with  $f_d T_s = 0.1$  (obviously with no interleaving).

For turbo coded experiments we use a rate-1/3 code with four-state constituent recursive convolutional codes with the generator function  $G(D) = (1, \frac{1+D^2}{1+D+D^2})$ . Fig-

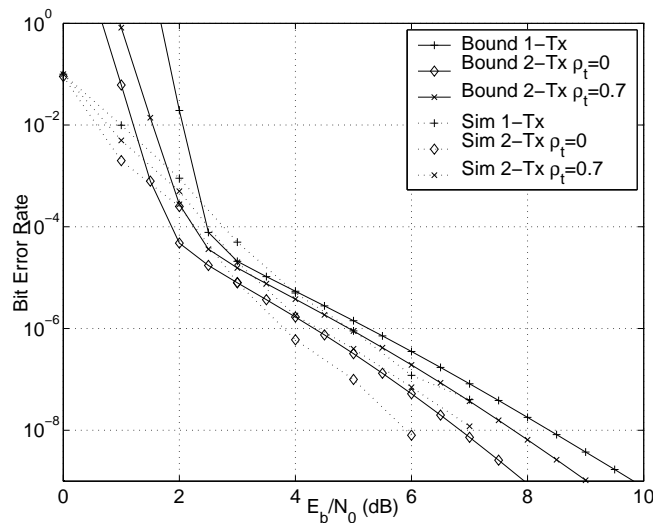


Figure 6.4. Turbo code, block i.i.d. Rayleigh Fading 2-Tx and 1-Rx antennas  $N=500$

Figure 6.4 shows the performance of turbo code concatenated with Alamouti signaling and one receive antenna. Each frame has 500 information bits (1500 BPSK symbols). We use suboptimal iterative (MAP) decoding of turbo codes with 12 iterations. The degradation due to transmit antenna correlation of  $\rho_t = 0.7$  is about 0.8 dB at  $\text{BER} = 10^{-7}$ . We see that the union bounds cross the simulation curves. This phenomenon, which has been previously reported in the literature [5], is due in part to the usage of iterative decoding instead of ML decoding. Figure 6.5 shows the performance of turbo code concatenated with Alamouti signaling and one receive antenna under quasi-static Rayleigh Channel. Each frame has 100 information bits (300 BPSK symbols). We use the limit before averaging method of [24] to obtain tighter bounds. The degradation due to transmit antenna correlation of  $\rho_t = 0.7$  is about 1.2 dB at  $\text{BER} = 10^{-3}$ .

Our TCM experiments use a code from [14] whose trellis is shown in Figure 6.6. In this experiment, the system has two transmit and one receive antenna, and frame length is 130 symbols (260 information bits). We have used partial input-output weight enumerating function (IOWEF) to calculate the upper bounds; the results

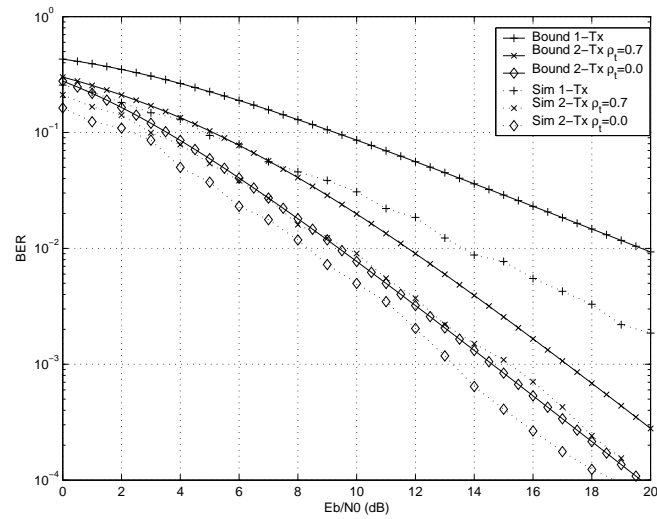


Figure 6.5. Turbo code, Quasi-static Rayleigh Fading 2-Tx and 1-Rx antennas,  $N=100$

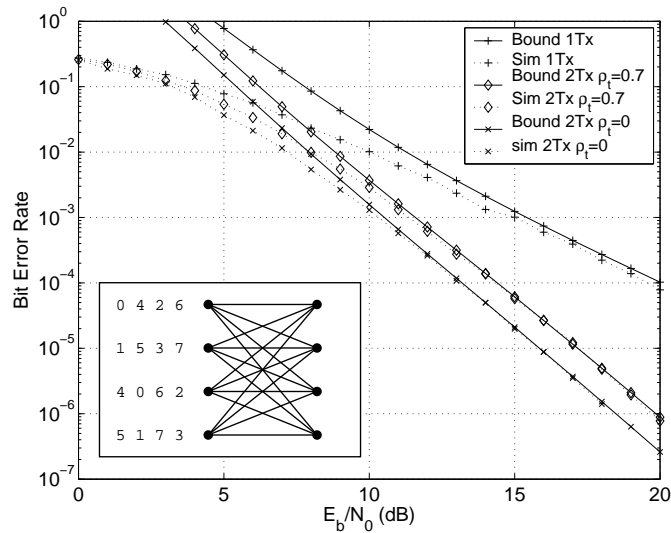


Figure 6.6. TCM, 2-Tx and 1-Rx antennas, block i.i.d. Rayleigh fading, BER

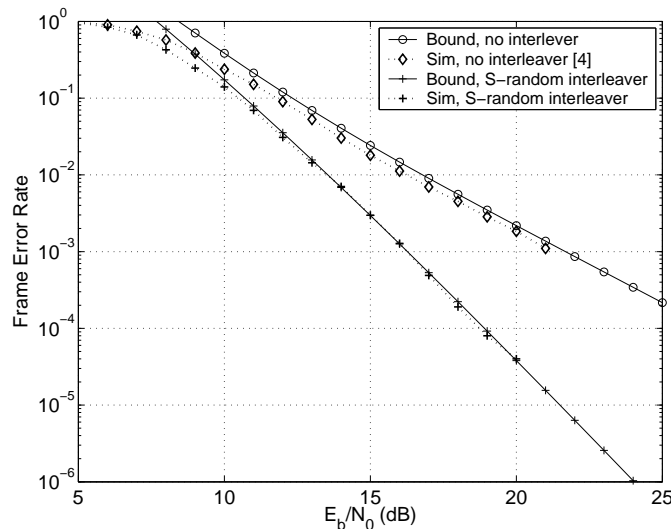


Figure 6.7. TCM, 2-Tx and 1-Rx antennas, block i.i.d. Rayleigh fading, FER

appear in Figure 6.6. The performance loss due to antenna correlation of  $\rho_t = 0.7$  is about 1.2 dB at  $\text{BER} = 10^{-5}$ .

To demonstrate the importance of interleaving, Figure 6.7 gives the frame error rate in the case of two transmit and one receive antennas under i.i.d. fading (conditions similar to [14]). We use a S-random interleaver with  $S=4$ . Interleaving gives a gain of 2.5 dB at  $\text{FER}=10^{-2}$ , in addition to a higher diversity that gives rise to even more impressive gains at higher SNR.

In Figure 6.8 we repeat the experiment under a *quasi-static* Rayleigh fading channel. The union bounds in the case of quasi-static channels are tight only if the diversity order is high, and the probability of deep fades is low [2]. To get a relatively tighter bound, we use the limit-before-averaging method of [24], but as reported in [24] the bounds are still not as tight as the fast fading bounds.

Our MTCM experiments use a 4-state, 8-PSK code from [19], concatenated with Alamouti signaling, with frame length of 100 symbols (200 information bits). Again, we use only the partial IOWEF to calculate upper bounds. Figure 6.9 shows

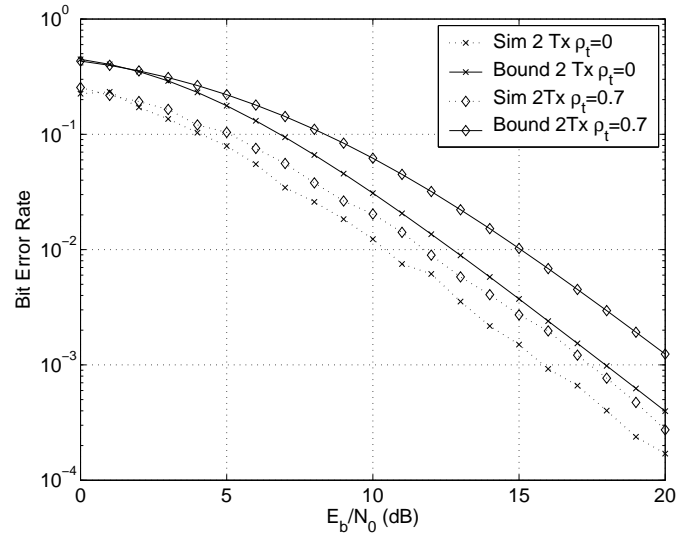


Figure 6.8. TCM, 2-Tx and 1-Rx antennas, quasi-static Rayleigh fading

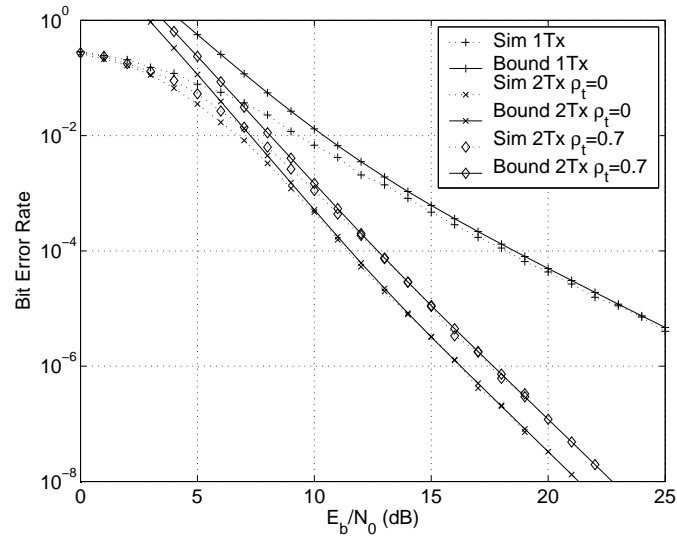


Figure 6.9. MTCM, 2-Tx and 1-Rx antennas, block i.i.d. Rayleigh Fading

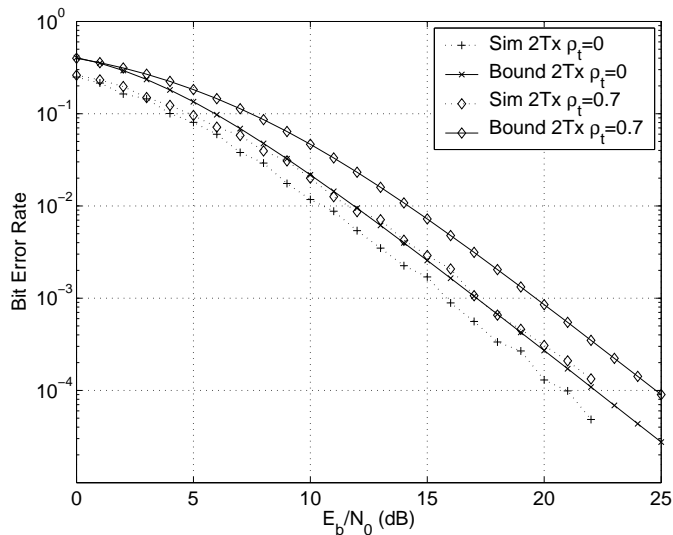


Figure 6.10. MTCM, 2-Tx and 1-Rx antennas, quasi-static Rayleigh Fading

that a spatial correlation of  $\rho_t = 0.7$  results in a 1dB loss at high SNR. We repeat this experiment under quasi-static fading (Figure 6.10). As mentioned before, the quasi-static bounds are not as tight as the fast fading bounds.

Finally, we show results for the performance of space-time coded TCM in Rician fading (Figure 6.11). The Rician fading parameter is  $K = 5dB$ , and there are two transmit and one receive antennas. The loss due to a transmit antenna correlation of  $\rho_t = 0.7$  is around 1dB.

## 6.2 Space-time codes

The PEP analysis of the previous section has wide applicability. In this section, we use PEP expressions to calculate union bounds for a variety of multiple-antenna signaling and coding schemes, including the space-time trellis (STT) codes [34], super-orthogonal space-time (SOSTT) codes [18] as well as linear dispersion (LD) codes [16]. Our results are also applicable, in a similar manner, to other signaling scenarios such as the diagonal algebraic space-time block codes [10].

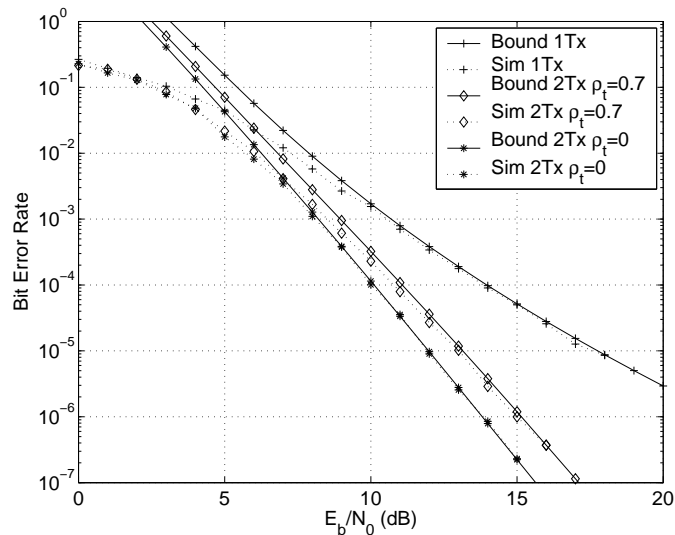


Figure 6.11. TCM, 2-Tx and 1-Rx antennas, block i.i.d. Rician fading  $K = 5dB$

The following expression gives the union bound for the frame error rate (FER) of the code in terms of the pairwise error probability

$$P_e \leq \sum_{\mathbf{x}} P(\mathbf{x}) \sum_{\hat{\mathbf{x}} \neq \mathbf{x}} P(\mathbf{x} \rightarrow \hat{\mathbf{x}}) , \quad (6.1)$$

where the multiplicity of the codewords are implicit in the inner summation. Bit-error rates (BER) can be obtained similarly. In general space-time signaling is nonlinear, thus it does not immediately follow that one can use the all-zero codeword as reference. However, in many cases, the symmetries in the code (and its corresponding trellis) leads to a condition where the error event probabilities as well as their multiplicities are independent of the transmitted codeword. This class, known as uniform error probability (UEP) codes [29], includes many of the interesting and practical scenarios. The past analyses have mostly relied on this property.

Interestingly, we found that transmit side correlation may destroy the UEP property of a code. Receive side correlation has no effect on UEP property. Thus, for the correlated case, one must take additional steps to simplify the analysis, as will be described in the sequel.

The evaluation of the union bound is possible via either the transfer function or the weight enumerating function. We use the partial weight enumerating function<sup>1</sup> of the codes for all our results.

Union bounds for the quasi-static channel are often loose, due to the fact that each codeword experiences only a single fading coefficient. To tighten the bounds, we use the limit before averaging method of Malkämaki and Leib [24]. Nevertheless, the bounds are still not as tight as the fast fading case, a fact widely recognized and reported. However, the union bounds will be tighter in the presence of diversity, i.e., when the probability of deep fades is relatively small. This can happen in MIMO channels, thus some of the quasi-static bounds are tighter than the SISO case.<sup>2</sup>

In the following figures, dashed lines denote simulations, while solid lines denote bounds. In the case of two antennas,  $\mathbf{R}_{\text{Tx}}$  and  $\mathbf{R}_{\text{Rx}}$  are each fully defined by a single correlation coefficient  $\rho_t$  for transmit antenna and  $\rho_r$  for receive antenna. When higher number of transmit or receive antennas are used, we consider the exponential correlation structure [29] which may correspond to the case of equi-spaced antennas with decaying factor  $\rho_r$ .

### 6.2.1 Space-time trellis codes

We present the results for space-time trellis codes in the context of the eight-state QPSK-STT code in [34], with spectral efficiency of 2 bit/sec/Hz and 130 information symbols per codeword (260 information bits).

The dominant error event for this trellis is shown in Figure 6.12, as well as the

---

<sup>1</sup>On the order of hundreds of error events were used for the union bounds reported in this work.

<sup>2</sup>In correlated channels, limit before averaging requires multidimensional integration of a non-linear function that, unlike the uncorrelated case, cannot be decomposed. We use Monte Carlo integration.

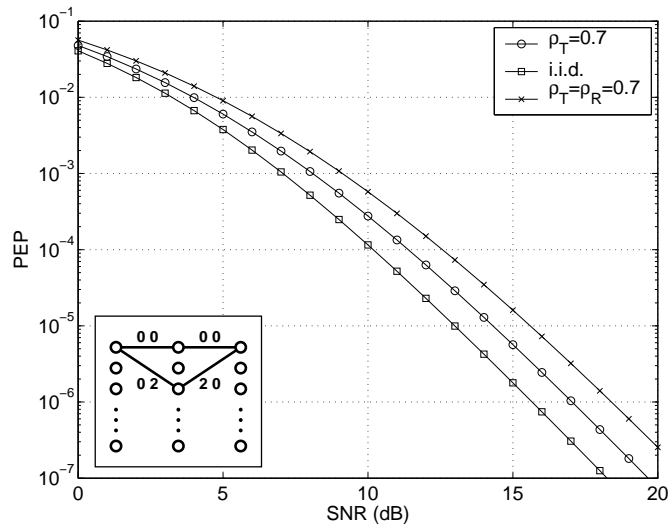


Figure 6.12. PEP of a dominant codeword, STT code, 2-Tx, 2-Rx, quasi-static Rayleigh fading

pairwise error probability (PEP) for the quasi-static channel under various spatial correlation situations. We notice that the diversity of the correlated cases are the same as the spatially uncorrelated case, since  $\mathbf{R}_{R_x}$  and  $\mathbf{R}_{T_x}$  are not rank deficient. But the correlation leads to a coding loss of over 1dB from  $\mathbf{R}_{T_x}$  and about 2.5dB when both transmit and receive side antennas are correlated.

Now we proceed to the calculation of the union bound. The eight-state STT code is a UEP code. However, when  $\mathbf{R}_{T_x} \neq \mathbf{I}$ , simulations show that, for example, the all-zero codeword and a random codeword experience different error rates, therefore the UEP property does not hold under spatially correlated fading. This surprising fact is demonstrated in Figures 6.13 and 6.15 for fast fading and quasi-static channels, respectively. In these two figures, we indicate the all-zero codeword with numeral (I), the codeword 02, 20, 02, 20, ... with numeral (II), and a random codeword with numeral (III).

This phenomenon can be explained as follows. When the channel is spatially uncorrelated, the phase of the received signals are random, so the signals from the

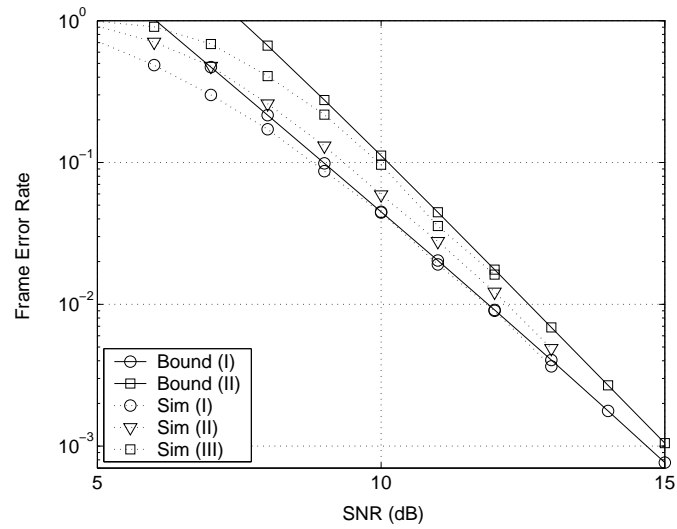


Figure 6.13. STT code, 2-Tx, 2-Rx, fast Rayleigh fading,  $\rho_t = \rho_r = 0.7$ , FER

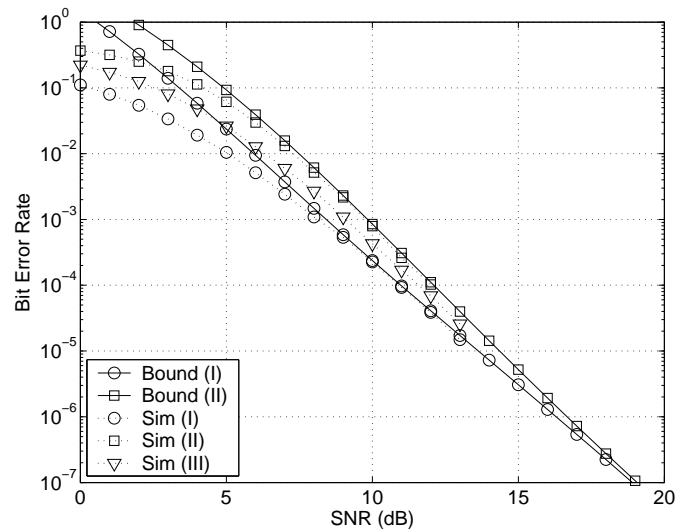


Figure 6.14. STT code, 2-Tx, 2-Rx, fast Rayleigh fading,  $\rho_t = \rho_r = 0.7$ , BER

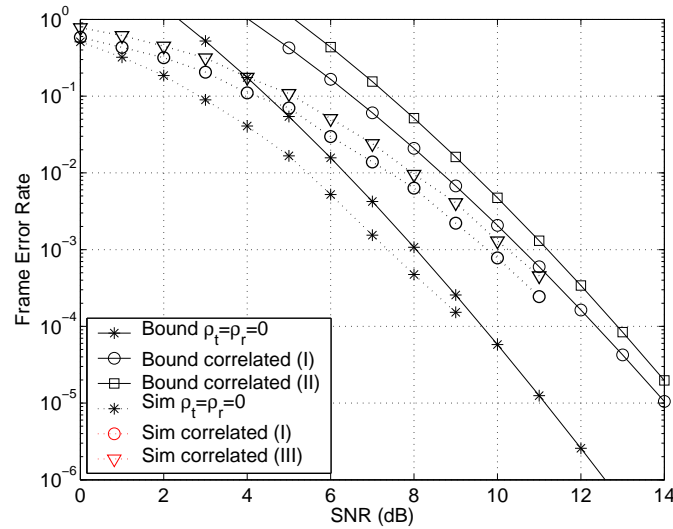


Figure 6.15. STT code, 2-Tx, 4-Rx, quasi-static Rayleigh fading,  $\rho_t = \rho_r = 0.7$

multiple transmit antennas may add constructively or destructively with equal probability. But when the channels are correlated, the signals from multiple transmit antennas are correlated. Assuming a positive correlation coefficient, this means that, in the case of two antennas, transmission vectors that send the same signal from two antennas (e.g. 00) have an advantage over vectors that send opposite values (e.g. 02 or 13 in QPSK). Worst-case codewords are those that are made entirely of these worst-case segments. Best case codewords are those made entirely of the same symbol, e.g., the all-zero codeword. A random codeword will contain a mixture of both, and therefore will fall somewhere in between.<sup>3</sup>

It is noteworthy that the loss of UEP property due to transmit antenna correlation is not universal. In the next section we demonstrate some codes that preserve their UEP property even if transmit antennas are spatially correlated.

Figure 6.13 shows frame error rates for the case of fast fading and two corre-

<sup>3</sup>In the presence of negative correlation, the role of best-case and worst-case codeword will be reversed.

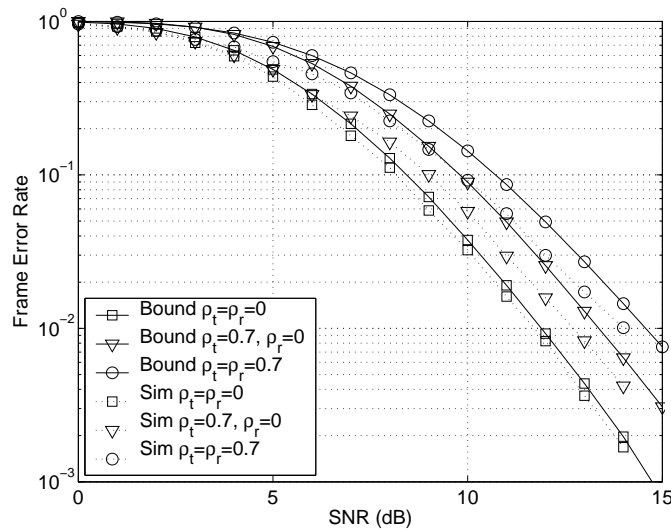


Figure 6.16. STT code, 2-Tx, 2-Rx, quasi-static Rayleigh fading

lated antennas ( $\rho_t = \rho_r = 0.7$ ). The frame error rates are calculated for the three cases of (I) all-zero codeword, (II) worst-case codeword, as mentioned above, and (III) random codeword. The three curves do not coincide and the UEP property does not hold. Figure 6.14 presents the BER results under the same conditions.

Now consider the performance of the space-time trellis code in quasi-static fading with four receive antennas (see Figure 6.15). The results for uncorrelated quasi-static channel are also included for comparison. We notice that the code has 2dB loss due to antenna correlation on transmit and receive sides.

The union bounds in Figure 6.15 is relatively tight, thanks to the high diversity. However, the union bound can be loose whenever diversity is low, e.g., if the number of receive antennas is small. In Figure 6.16, we present the performance of the STT code with two receive antennas with tight union bounds calculated using the limit-before-averaging method. For spatially correlated cases, we present the union bound for the worst case reference codeword, as described earlier. Simulations are performed, naturally, with random inputs. For this reason, the bounds for the correlated cases

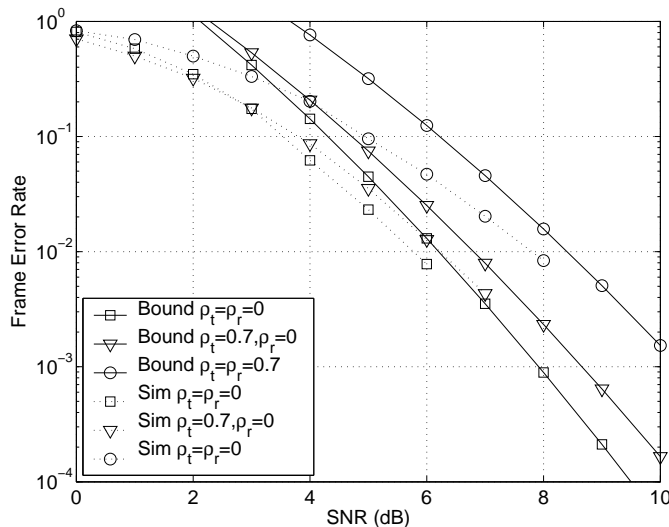


Figure 6.17. STT code, 2-Tx, 4-Rx, temporally correlated Rayleigh fading,  $f_d T_s = 0.01$

are not as tight. The performance of the STT code with four receive antennas in a temporally and spatially correlated channel is presented in Figure 6.17.

### 6.2.2 Super-orthogonal space-time trellis codes

Simon and Jafarkhani [30] analyzed the performance of SOSTT codes under spatially and temporally uncorrelated channel, for which they developed a specialized analysis. Unlike [30], we evaluate the performance of a SOSTT with the same PEP expressions reported in Chapter 4 simply by a change of notation as follows. The subscript  $n$  in (4.1) and in the definition of  $\mathbf{x}_n$  and  $\Delta_n$  now stands for the  $n$ -th time-interval with length  $n_T$ , i.e., the  $n$ -th trellis section. For example, for  $n_T = 2$ , we have

$$\Delta_n = \mathbf{x}_n - \hat{\mathbf{x}}_n = \begin{pmatrix} x_{n,1}e^{j\theta_n} - \hat{x}_{n,1}e^{j\hat{\theta}_n} & -x_{n,2}^*e^{j\theta_n} + \hat{x}_{n,2}^*e^{j\hat{\theta}_n} \\ x_{n,2} - \hat{x}_{n,2} & x_{n,1}^* - \hat{x}_{n,1}^* \end{pmatrix}, \quad (6.2)$$

where  $x_{n,1}$  and  $x_{n,2}$  are the two signals transmitted by the STB code in the  $n$ -th trellis section, and  $\theta_n$  is the corresponding phase shift, which depends on the encoder state. Using this modification, the PEP when in each trellis section (i.e. each block)

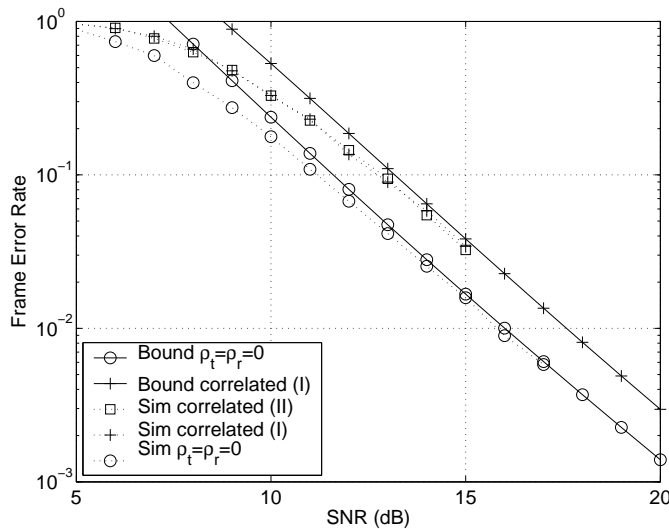


Figure 6.18. SOSTT code, 2-Tx, 1-Rx, fast Rayleigh fading,  $\rho_t = 0.7$

is given by Equation (4.16). This change of notation does not affect the results for the quasi-static channel.

Our analysis applies to any SOSTT code, but for demonstration purposes we consider the two-state SOSTT code [18] with  $n_T = 2$  and BPSK modulation, which has a spectral efficiency of 1 bit/sec/Hz. Unlike the STT code in Section 6.2.1, this code preserves its UEP property even when  $\mathbf{R}_{T_x} \neq \mathbf{I}$ , because all trellis paths transmit STB codewords that are symmetric with respect to spatial correlations, therefore they are all affected similarly. This may not be true for all block space-time codes, however. The results for fast Rayleigh fading for one receive antenna are shown in Figure 6.18. The numeral (I) refers to the all-zero transmitted codeword, and (II) refers to a random codeword. Simulations show no difference, thus confirming UEP property. For comparison, the results for spatially independent fast fading are presented. We see a loss of about 2dB in coding gain due to transmit-side correlation, but no change in diversity.

The performance of the SOSTT code with four receive antennas in a quasi-

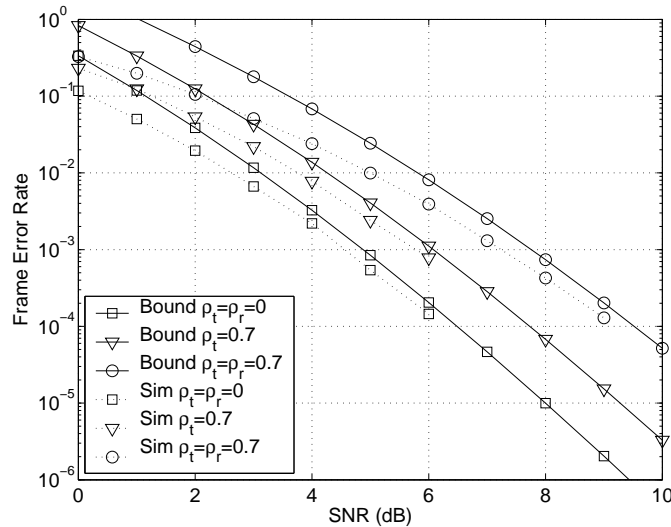


Figure 6.19. SOSTT code, 2-Tx, 4-Rx, quasi-static Rayleigh fading,  $\rho_t = \rho_r = 0.7$

static, spatially correlated channel is shown in Figure 6.19 and for temporally and spatially correlated channel is presented in Figure 6.20.

### 6.2.3 Linear-dispersion codes

LD codes in general do not have the UEP property. The UEP property arises from the symmetry of the code, and general LD codes do not possess a structure that imparts such symmetry. Therefore, even though the PEP expressions derived earlier are useful, for an estimate of the error rate (union bound) all possible codeword pairs must be considered.

For our examples we choose LD codes with  $n_T = 2$ ,  $n_R = 2$ , and  $T = 2$ . This LD code with  $Q = n_T \times T = 4$  is reported in [16] and its performance evaluated with QPSK and 16-QAM constellations. We apply the block fading model, i.e., fixed fading coefficient over each block, varying independently between blocks. First consider QPSK, which leads to 256 codewords and a rate of 4 bits/sec/Hz. The simulated and analytical FER results of this code are shown in Figure 6.21 for uncorrelated as

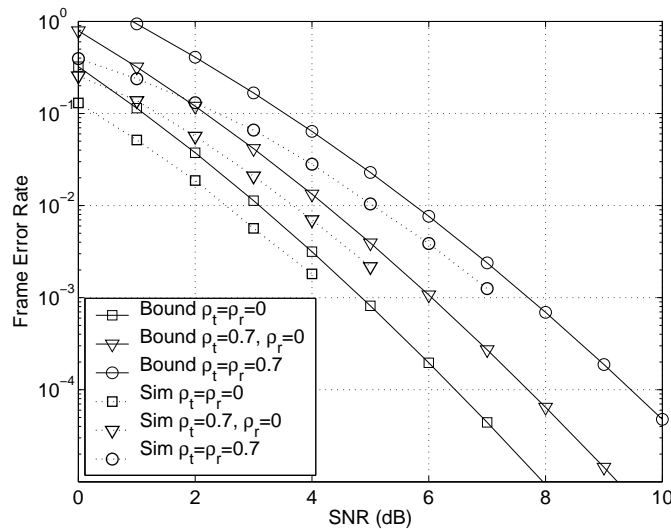


Figure 6.20. SOSTT code, 2-Tx, 4-Rx, temporally correlated Rayleigh fading,  $f_d T_s = 0.01$

well as spatially correlated antennas. When correlation exists in both transmit and receive sides the loss in performance is about 3dB.

Using 16-QAM with the same structure leads to spectral efficiency of 8 bits/sec/Hz and 65536 codewords. For the calculation of a union bound for a given codeword, 65535 errors are considered. But most of these errors are low-probability and highly statistically dependent, resulting in a loose union bound. A better approximation can be found by concentrating on the closest codewords that constitute most of the error probability. For a given codeword  $\mathbf{X}(x_1, \dots, x_Q)$  there are 256 neighboring codewords whose uncoded sequences are different in only one  $x_i$ , and that one  $x_i$  is separated in the two codewords only by the minimum Euclidean distance of 16-QAM. In a sense, we have 256 “nearest” codewords, and we can use them in calculating the error performance. The results are shown in Figure 6.22, where the numeral (I) refers to the union bound and numeral (II) refers to the truncated bound.<sup>4</sup> The performance figures can

<sup>4</sup>In the LD code experiments, we randomly choose reference codewords until the calculated union bound converges. For the 16-QAM experiment, 50 reference codewords proved to be sufficient.

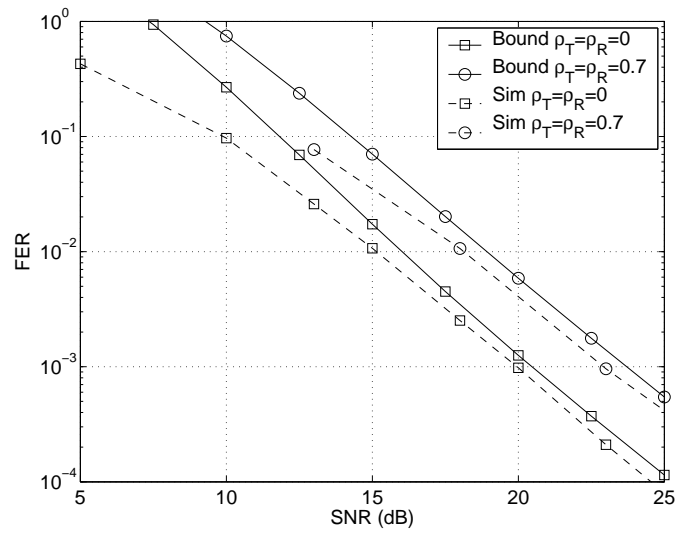


Figure 6.21. LD code, 2-Tx, 2-Rx, QPSK, Rayleigh fading

be made even tighter in the low-SNR region by applying the limit-before-averaging technique of [24], at the cost of some computational inconvenience.

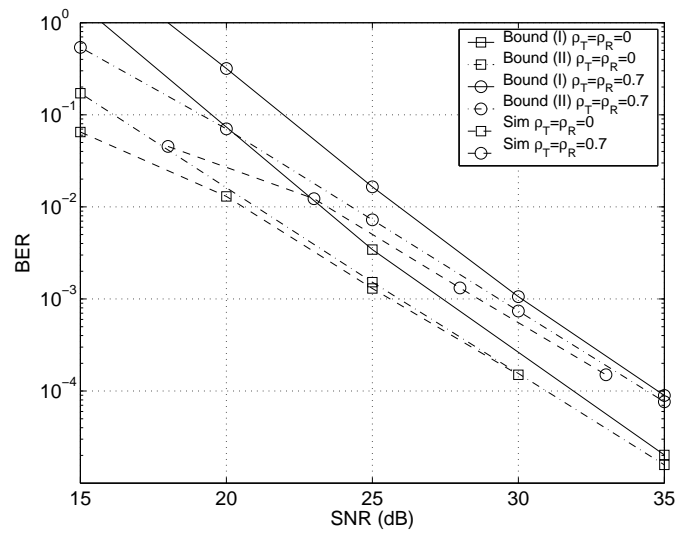


Figure 6.22. LD code, 2-Tx, 2-Rx, 16QAM, Rayleigh fading

## CHAPTER 7

### CONCLUSION AND FUTURE WORK

In this thesis, we provide analysis of space-time codes. Our analysis is applicable to all space-time code under realistic channel conditions. Especially, we consider the effects of spatial and temporal correlation in channel on space-time codes. Previously presented results for independent channels and quasi-static or fast fading are special cases of our results. We provide results Rayleigh as well as Rician fading. We consider the effects of block fading and interleaving.

We start in Chapter 3 by presenting existing tools that applies to our analysis. Of particular interest is the spatially correlated channel model which is based on the transmit and receive antenna correlation. We explain exact expression for Q-function and union bounds using weight enumerating functions. We also show how the problem of finding union bounds is reduced to problem of finding moment generating function (characteristic function) of SNR under various channel conditions.

In Chapter 4 we present analysis of space-time codes. We use a mathematical result that gives characteristic function of a quadratic form to find the moment generating function for various cases. We consider quasi-static as well as fast fading spatially correlated channels. Furthermore, we also consider a case where fading is constant over a block, but varies independently from block to block, known as block fading. In section 4.5 we provide results for general temporal and spatial correlation. In section 4.6 we present the analysis for Rician channels. It can be shown that the previous cases are special case of this last expression.

In Chapter 5 we give analysis for the special case of coded space-time block transmission. Space-time block codes offer diversity gain, but no coding gain. It is advantageous to concatenate channel codes with space-time block codes to improve system performance. This scheme is practically attractive, and has been adopted in WCDMA. To derive the moment generating functions, we use uniform transformation on the correlated channel. We consider the effects of interleaving. We also consider effects of block fading assumption inherent in space-time block codes. However, interleaving makes the analysis difficult in presence of block fading channels. We solve this problem by using the concept of “uniform interleaving”. Using this concept, we average over all possible interleavers. We show that this concept makes analysis easier, yet provides tight bounds. Similar to the case of space-time codes, we give analysis of coded space-time block transmission for spatially as well as temporally correlated channel. We give analysis for BPSK as well as multilevel modulation.

In Chapter 6, we compare the analytical bounds with simulation results. We show plots for space-time trellis codes, super-orthogonal space-time codes and linear-dispersion codes, however we note that our analytical expressions are applicable to other space-time codes as well. The analytical bounds are based on partial weight enumerating function. For the case of coded space-time block transmission, we give plots for convolutional codes, turbo codes, TCM and MTCM. For the cases of convolutional codes, and turbo codes, we use full weight enumerating function. But for TCM and MTCM, we use partial weight enumerating function. We note that the bounds are tight in fast fading channel. The bounds in quasi-static channel are loose because there is no dominant error event in quasi-static channel. We note that for higher diversity, the bounds in quasi-static channel are tighter than bounds for lower diversity. In quasi-static channels, we use the method of limit-before-averaging to tighten the bounds.

One of the direct extension of this work can be design of space-time codes for spatially correlated channels. From the analytical equations, we see that the performance depends on the ranks of transmit and receive correlation matrices. Water-filling can be one of the solutions to take advantage of correlations in low to medium SNR range.

In the analysis we assume perfect channel estimation. In practice, channel estimation is either absent or imperfect. It would be interesting to analyze space-time coding for imperfect or blind channel estimation. We also assume frequency non-selective fading. If the channel is frequency selective, one can use OFDM-STTC. The analysis of this system can give some useful insights into designing codes for frequency selective channels.

One of the interesting observations in this chapter is the destruction of uniform error probability property of space-time trellis codes in presence of antenna correlation. It is possible to design space-time trellis codes that preserve uniform error probability property even under spatial correlation.

## BIBLIOGRAPHY

- [1] S. M. Alamouti, “A simple transmit diversity technique for wireless communications,” *IEEE J. Select. Areas Commun.*, vol. 16, no. 8, pp. 1451–1458, October 1998.
- [2] G. Bauch and J. Hagenauer, “Analytical evaluation of space-time transmit diversity with FEC-coding,” in *Proc. IEEE GLOBECOM*, San Antonio, TX, November 2001, pp. 435–439.
- [3] —, “Smart versus dumb antennas-capacities and FEC performance,” *IEEE Communications Letters*, vol. 6, no. 2, pp. 55–57, Feb. 2002.
- [4] G. Bauch, J. Hagenauer, and N. Seshadri, “Turbo processing in transmit antenna diversity systems,” *Ann. Telecommun.*, vol. 56, no. 7–8, pp. 455–471, 2001.
- [5] S. Benedetto, D. Divsalar, G. Montorsi, and F. Pollara, “Serial concatenation of interleaved codes: performance analysis, design, and iterative decoding,” *IEEE Trans. Inform. Theory*, vol. 44, no. 3, pp. 909–926, May 1998.
- [6] S. Benedetto and G. Montorsi, “Unveiling turbo codes: Some results on parallel concatenated coding schemes,” *IEEE Trans. Inform. Theory*, vol. 42, no. 2, pp. 409–428, March 1996.
- [7] H. Bölcskei and A. J. Paulraj, “Performance of space-time codes in the presence of spatial fading correlation,” in *Proc. Asilomar Conference on Signals, Systems and Computers*, October 2000, pp. 687–693.

- [8] M. Borran, M. Memarzadeh, and B. Aazhang, "Design of coded modulation schemes for orthogonal transmit diversity," submitted for publication in *IEEE transaction on Communications*, May 2001.
- [9] C. Chuah, D.Tse, J. Kahn, and R. Valenzuela, "Capacity scaling in MIMO wireless systems under correlated fading," *IEEE Trans. Inform. Theory*, vol. 48, no. 3, pp. 637–650, March 2002.
- [10] M. O. Damen, K. Abde-Meraim, and J. C. Belfiore, "Diagonal algebraic space-time block codes," *IEEE Transactions on Information Theory*, vol. 48, no. 3, pp. 938–952, March 2002.
- [11] M. Damen, A. Abdi, and M. Kaveh, "On the effect of correlated fading on several space-time coding and detection schemes," in *Proc. IEEE Vehicular Technology Conference*, 2001, pp. 13–16.
- [12] G. Foschini, "Layered space-time architecture for wireless communication in a fading environment when using multi-element antennas," in *Bell Labs Technical Journal*, 1996, pp. 41–59.
- [13] G. Foschini and M. Gans, "On limits of wireless communication in a fading environment when using multiple antennas," *Wireless Personal Communications*, vol. 6, pp. 311–335, March 1998.
- [14] Y. Gong and K. B. Letaief, "Concatenated space-time block coding with trellis coded modulation in fading channels," *IEEE Transactions on Wireless Communications*, vol. 1, no. 4, pp. 580–590, Oct 2002.
- [15] L. Hanzo, T. Liew, and B. Yeap, *Turbo Coding, Turbo Equalisation and Space-Time Coding for Transmission over Fading Channels*. New York: John Wiley and Sons, 2002.

- [16] B. Hassibi and B. Hochwald, "High-rate codes that are linear in space and time," *IEEE Transactions on Information Theory*, vol. 48, no. 7, pp. 1804–1824, July 2002.
- [17] A. Hedayat, H. Shah, and A. Nosratinia, "Analysis of space-time coding in correlated fading channels," *submitted to IEEE Transactions on Wireless Communications*, 2003.
- [18] H. Jafarkhani and N. Seshadri, "Super-orthogonal space-time trellis codes," *IEEE Transactions on Information Theory*, vol. 49, no. 4, pp. 937–950, April 2003.
- [19] S. H. Jamali and T. Le-Ngoc, *Coded Modulation Techniques for Fading Channels*. Massachusetts: Kluwer Academic Publishers, 1994.
- [20] R. Knopp and P. A. Humblet, "On coding for block fading channels," *IEEE Trans. Inform. Theory*, vol. 46, no. 1, pp. 189–205, Jan 2000.
- [21] J. Lai and N. B. Mandayam, "Performance of turbo coded WCDMA with down-link space-time block coding in correlated fading channels," accepted for publication in *IEEE transaction on wireless communications*, 2002.
- [22] E. G. Larsson and P. Stoica, *Space-Time Block Coding for Wireless Communications*. Cambridge, UK: Cambridge University Press, 2003.
- [23] K. Liu and A. M. Sayeed, "Space-time code design for correlated MIMO channels," in *Proceedings of the 40th Annual Allerton Conference on Communication, Control and Computing*, Monticello, Illinois, USA, October 2002.
- [24] E. Malkamäki and H. Leib, "Evaluating the performance of convolutional codes over block fading channels," *IEEE Trans. Inform. Theory*, vol. 45, no. 5, pp. 1643–1646, July 1999.

- [25] J. G. Proakis, *Digital Communications*, 3rd ed. New York: McGraw-Hill, 1995.
- [26] H. Schulze, “Performance analysis of concatenated spacetime coding with two transmit antennas,” *IEEE Transactions on Wireless Communications*, vol. 2, no. 4, pp. 669–679, July 2003.
- [27] H. Shah, A. Hedayat, and A. Nosratinia, “Performance of concatenated channel codes and orthogonal space-time block codes,” *submitted to IEEE Transactions on Wireless Communications*, 2003.
- [28] M. K. Simon, “Evaluation of average bit error probabilities for space-time coding based on a simpler exact evaluation of pairwise error probability,” *Journal of Communications and Networks*, vol. 3, no. 3, pp. 257–264, September 2001.
- [29] M. K. Simon and M.-S. Alouini, *Digital Communication over Fading Channels: A Unified Approach to Performance Analysis*. New York: John Wiley and Sons, 2000.
- [30] M. K. Simon and H. Jafarkhani, “Performance evaluation of super-orthogonal space-time trellis codes using a moment generating function-based approach,” *accepted, IEEE Transaction on Signal Processing*, 2003.
- [31] G. L. Stüber, *Mobile Communication*. Kluwer Academic Publishers, 2001.
- [32] V. Tarokh, H. Jafarkhani, and A. Calderbank, “Space-time block codes from orthogonal designs,” *IEEE Trans. Inform. Theory*, vol. 45, no. 5, pp. 1456–1467, July 1999.
- [33] —, “Space-time block coding for wireless communications: Performance results,” *IEEE Trans. Inform. Theory*, vol. 45, no. 5, pp. 1456–1467, July 1999.

- [34] V. Tarokh, N. Seshardi, and A. Calderbank, “Space-time codes for high data rate wireless communication: Performance criteria and code construction,” *IEEE Trans. Inform. Theory*, vol. 44, no. 2, pp. 744–765, March 1998.
- [35] G. L. Turin, “The characteristic function of Hermetian quadratic forms in complex normal random variables,” *Biometrika*, pp. 199–201, June 1960.
- [36] M. Uysal and C. Georghiades, “On the error performance analysis of space-time trellis codes: an analytical framework,” in *Proc. IEEE Wireless Communications and Networking Conference WCNC*, 2002, pp. 99–104.
- [37] —, “Upper bounds on the BER performance of MTCM-STBC schemes over shadowed Rician fading channels,” in *Proc. IEEE Vehicular Technology Conference*, 2002, pp. 62–66.
- [38] S. A. Zummo and W. E. Stark, “Performance analysis of coded systems over block fading channels,” in *Proc. IEEE Vehicular Technology Conference*, 2002, pp. 1129–1133.

## VITA

Harsh Shah, was born in Ahmedabad, India, on 18 December 1978, the son of Kaumudi Shah and Piyush Shah. He finished high school studies in 1996 at A.G. Teachers' High School, Ahmedabad, India. He received Bachelor of Engineering in Electronics and Communications from Gujrat University, Ahmedabad, India, in June 2001. He joined the master's program in Electrical Engineering at the University of Texas at Dallas, Richardson, USA in August 2001.

Permanent address: 7, Boscovilla  
Nehrupark, Vastrapur  
Ahmedabad, Gujarat - 380015  
India

This thesis was typeset with L<sup>A</sup>T<sub>E</sub>X<sup>†</sup> by the author.

---

<sup>†</sup>L<sup>A</sup>T<sub>E</sub>X is a document preparation system developed by Leslie Lamport as a special version of Donald Knuth's T<sub>E</sub>X Program.